MR Thermometry

Le Zhang

M229

May 15, 2018

David Geffen School of Medicine

UCLA Magnetic Resonance Research Labs

UCLA Radiology

Why Thermometry with MR?

- Accurate temperature measurement is critical for successful implementation of thermal therapies

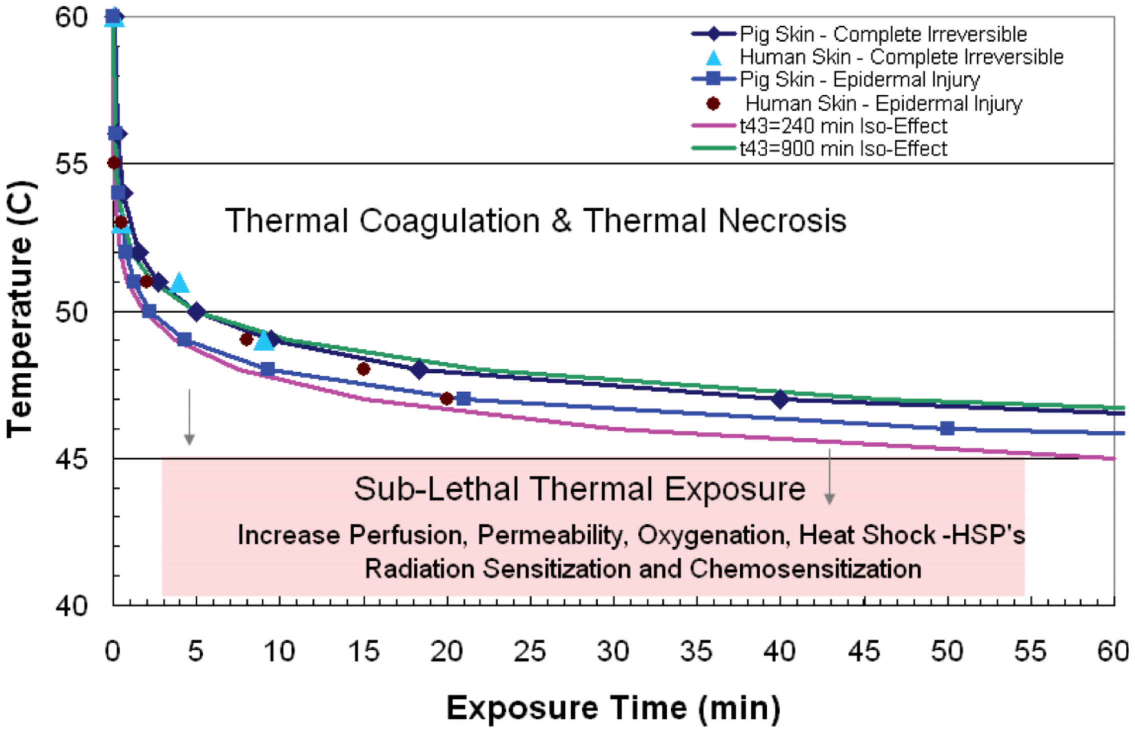

David Geffen School of Medicine

Diederich, CJ, *Int. J. Hyperthermia*, 2015

Why Thermometry with MR?

- During High-Intensity Focused Ultrasound (HIFU) treatment sessions, it is even more important to be able to relate treatment temperature to actual thermal tissue damage

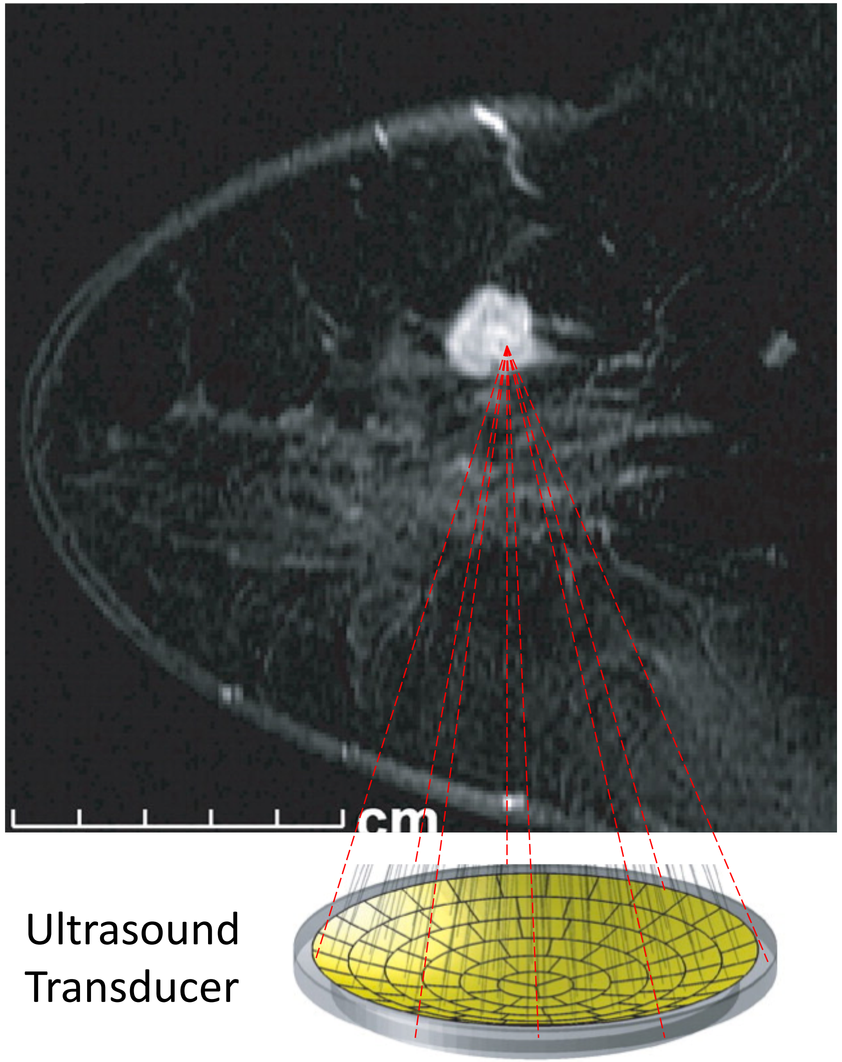

Tempeny, CMC, *Radiology*, 2011

Why Thermometry with MR?

- Invasive thermometry methods can have severe complications such as hemorrhage, infections and/or pain

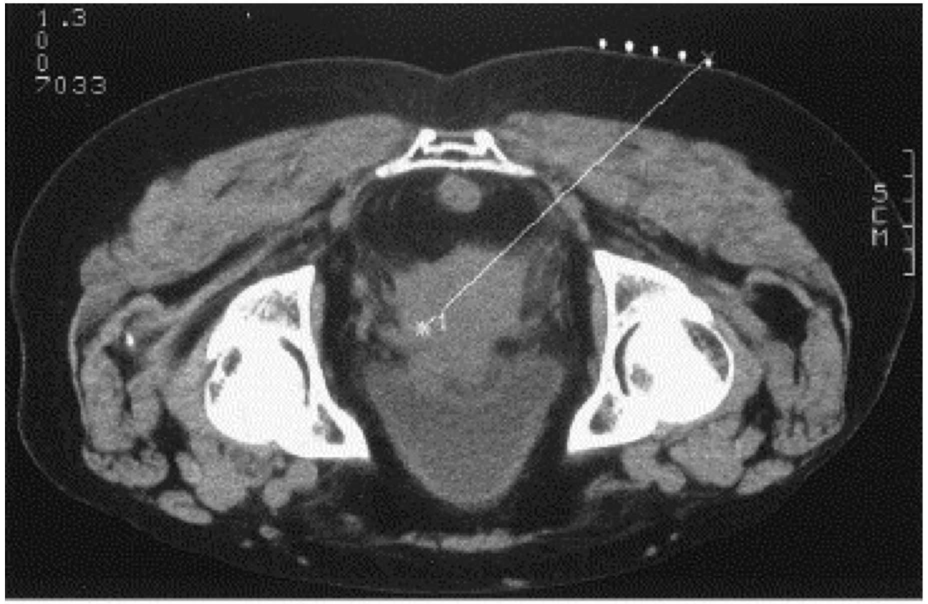

CT-guided Insertion of Thermal Probe

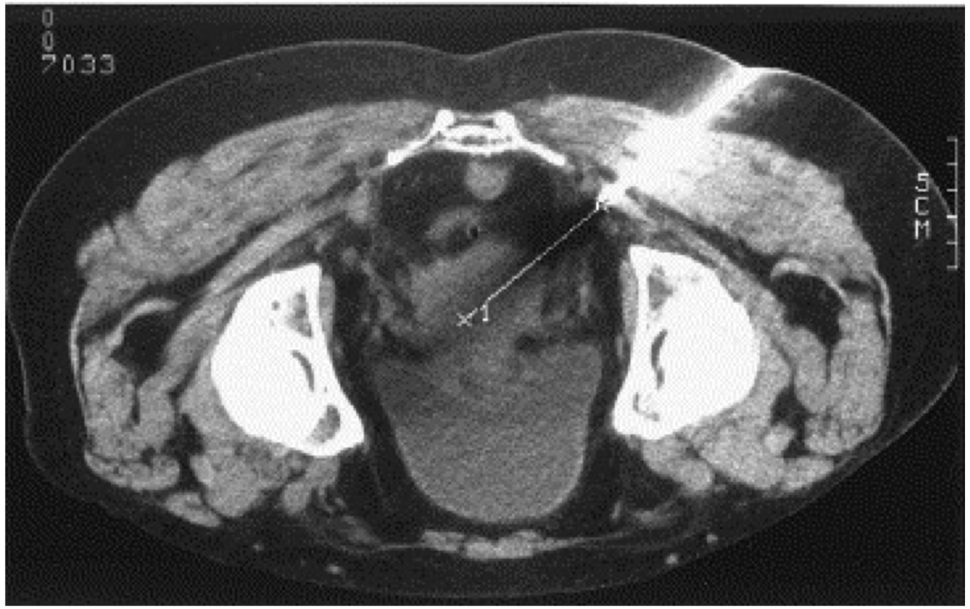

van der Zee, J, *Int J Radiat Oncol Biol Phys*, 1998

Why Thermometry with MR?

- MRI has a wider coverage, and it can also provide anatomical references to guide treatment

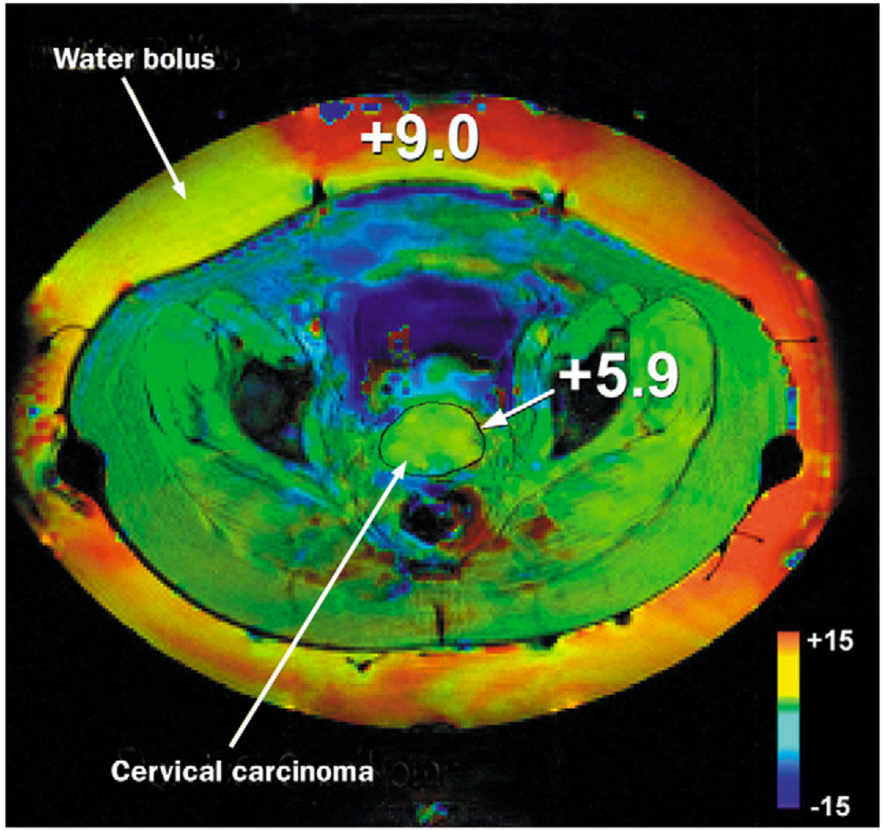

David Geffen School of Medicine

Wust, P, *Lancet Oncol*, 2002

MRI: What to Measure Temperature With?

What contrast does MRI provide?

- Proton density
- T_1
- T_2
- T_2^*
- Apparent diffusion coefficient
- Chemical shift
- Magnetization transfer

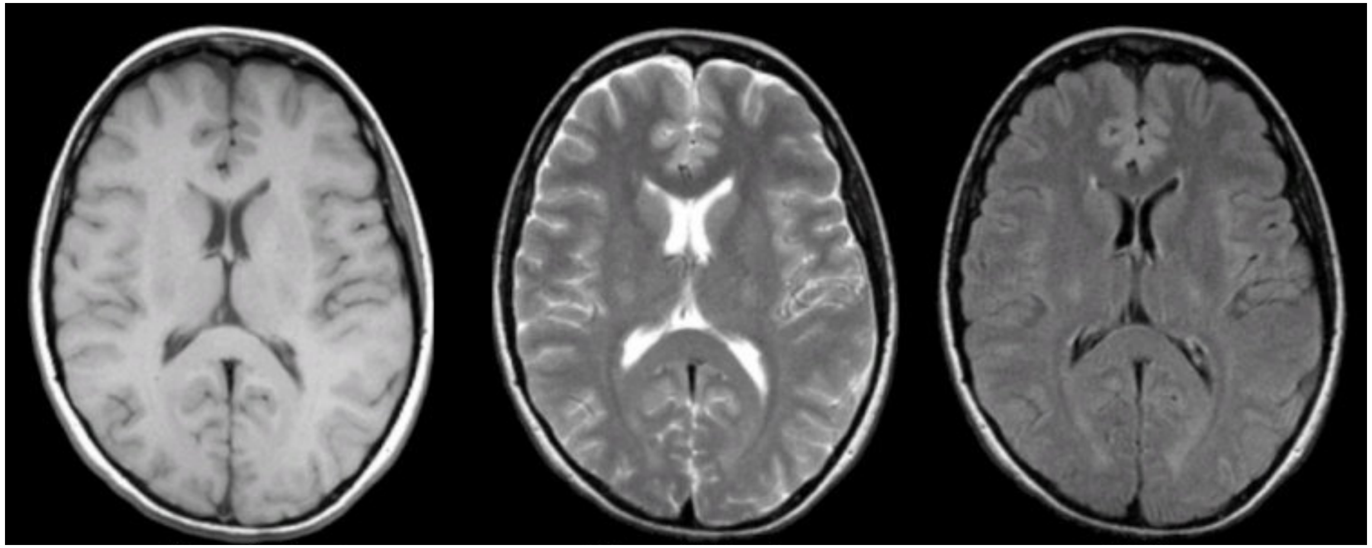

Turns out, they are all temperature dependent!

MR Thermometry with Proton Density

- Proton density (M_0) obeys Boltzmann Distribution

$$M_0 = N\frac{\gamma^2 h^2 B_0}{4\mu_0 kT} \propto \frac{1}{T}$$

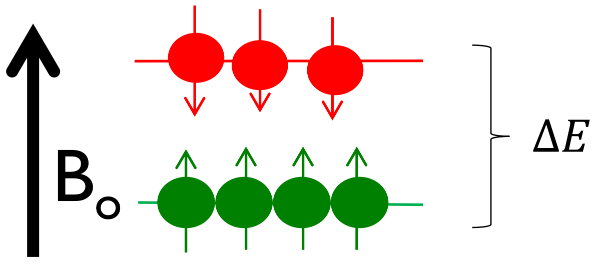

- Between 37 and 80°C, PD decreases linearly with temperature at a rate of (-0.30±0.01)%/°C

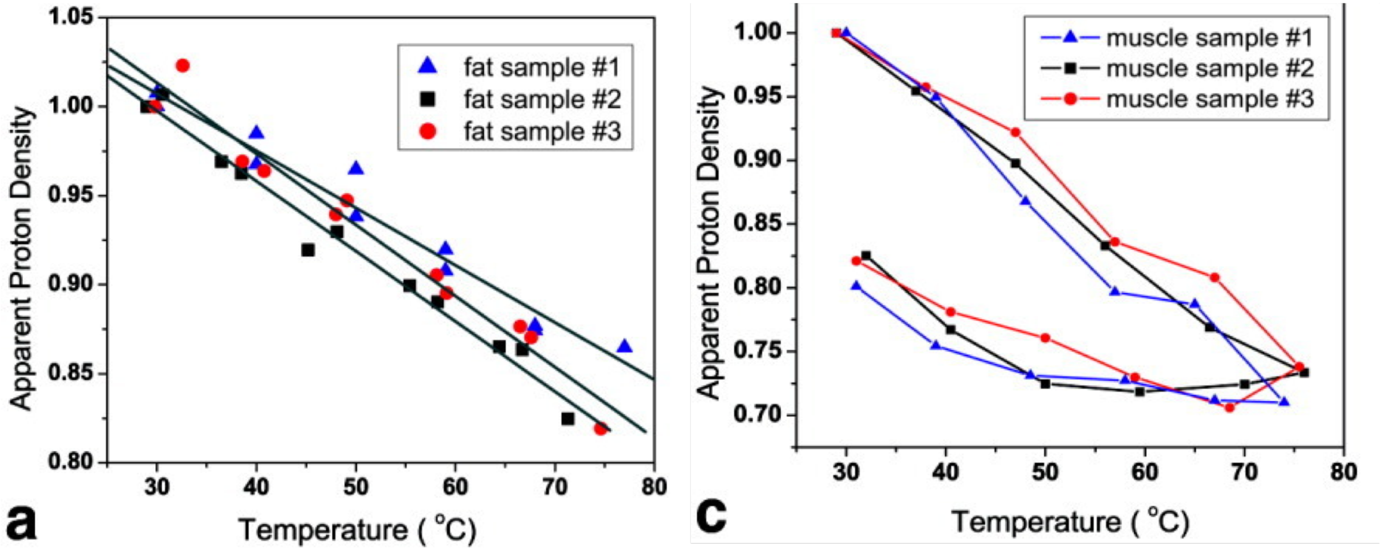

Chen J. *J Magn Reson Imaging*, 2006

David Geffen School of Medicine

MR Thermometry with T_1

- The spin-lattice relaxation stems from the dipolar interaction between molecules, a process that requires overcoming an activation energy E_a

$$T_1(T) \propto e^{-E_a(T_1)/kT} \approx T_1\left(T_{ref}\right) + m \cdot (T - T_{ref})$$

- The temperature coefficient is determined empirically for different tissue types. T_1 generally increases by 1%/°C, with some tissue variation

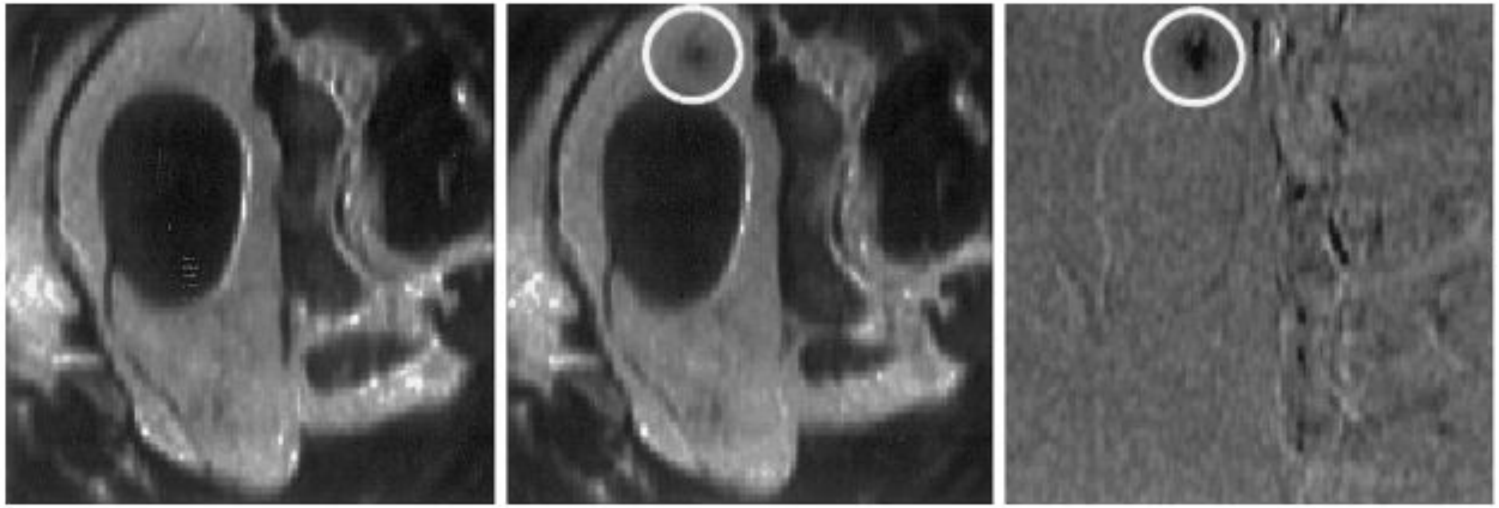

David Geffen School of Medicine

Hynynen K, *Magn Reson Med* 2000

MR Thermometry with T_1: Weighted Imaging

- For both spin echo and gradient echo sequences, the change in T_1 signal intensity at an unknown temperature T with respect to a reference temperature T_{ref} due to temperature can be modeled as

$$\frac{\mathrm{d}S}{S\mathrm{d}T} = -\frac{m\mathrm{TR}(1-cos\alpha)E_1}{T_1 T_{ref}^2(1-E_1)(1-E_1 cos\alpha)} - \frac{1}{T_{ref}}$$

where

$$E_1 = \exp[-\frac{TR}{T_1 T_{ref} + m(T - T_{ref})}]$$

MR Thermometry with T_1: Mapping Method

- T_1 can be determined by using inversion-recovery method, but it can be very time-consuming.
- The temperature dependence of T_1 is also varies with tissue type.

Table 2. T_1 temperature dependence (in ms/°C) at a given initial temperature T_0. For the individual samples, '±' denotes the standard deviation (n = 30) over the voxels of the region of interest (ROI). For the average value, '±' denotes the standard deviation over the mean of the seven samples

Sample	T_0 = 25 °C	T_0 = 35 °C	T_0 = 45 °C	T_0 = 55 °C	T_0 = 65 °C
1, heating	5.39 ± 0.09	6.28 ± 0.14	7.23 ± 0.20	8.24 ± 0.27	9.30 ± 0.36
1, cooling	5.38 ±0.10	6.26 ±0.13	7.20 ±0.16	8.20 ± 0.21	9.25 ± 0.27
1, extracted fat	5.48 ±0.12	6.41 ± 0.18	7.41 ±0.25	8.47 ± 0.33	9.60 ± 0.43
2, heating	5.45 ± 0.07	6.39 ± 0.14	7.41 ± 0.24	8.49 ± 0.36	9.64 ± 0.50
3, heating	5.25 ± 0.14	6.23 ± 0.22	7.29 ± 0.31	8.44 ± 0.43	9.67 ± 0.58
4, heating	5.40 ± 0.05	6.35 ± 0.12	7.38 ± 0.10	8.47 ± 0.15	9.63 ± 0.21
4, cooling	5.40 ± 0.09	6.27 ± 0.12	7.20 ± 0.17	8.18 ± 0.23	9.21 ± 0.31
5, heating	5.24 ± 0.15	6.14 ± 0.20	7.10 ± 0.27	8.13 ± 0.35	9.22 ± 0.45
6, heating	5.34 ± 0.06	6.28 ± 0.09	7.31 ± 0.13	8.40 ± 0.19	9.57 ± 0.27
7, heating	5.36 ± 0.09	6.30 ± 0.14	7.32 ± 0.21	8.41 ± 0.28	9.57 ± 0.37
Average (n = 7) (of heating)	5.35 ± 0.08	6.28 ± 0.08	7.29 ± 0.09	8.36 ± 0.12	9.50 ± 0.16

Baron P, *NMR Biomed* 2015

MR Thermometry with T_1: Mapping Method

- Variable flip angle (VFA) method can serve as a faster alternative for T_1 mapping
  - Flip angles are chosen such that they generate 70% of the Ernst angle signal magnitude, enabling faster mapping
  - B_1 map is required to correct for flip angle errors
  - T_1 can be calculated by fitting the MR signal intensity and flip angle ϑ with

$$S = M_0 \frac{\left(1 - e^{-TR/T_1}\right) sin\theta}{1 - e^{-TR/T_1} e^{-TR/T_2^*} - \left(e^{-TR/T_1} - e^{-TR/T_2^*}\right) cos\theta}$$

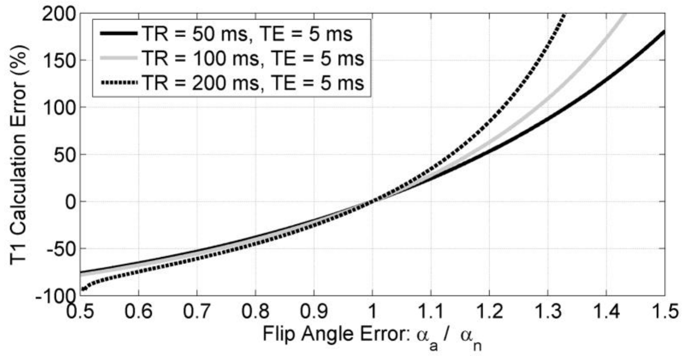

T_1 Error Caused by Imperfect Flip Angle

Todd N, *Magn Reson Med*, 2013

MR Thermometry with T_1: Steady State

We record M_x, M_y and Mz as a ratio against the initial magnetization M_0

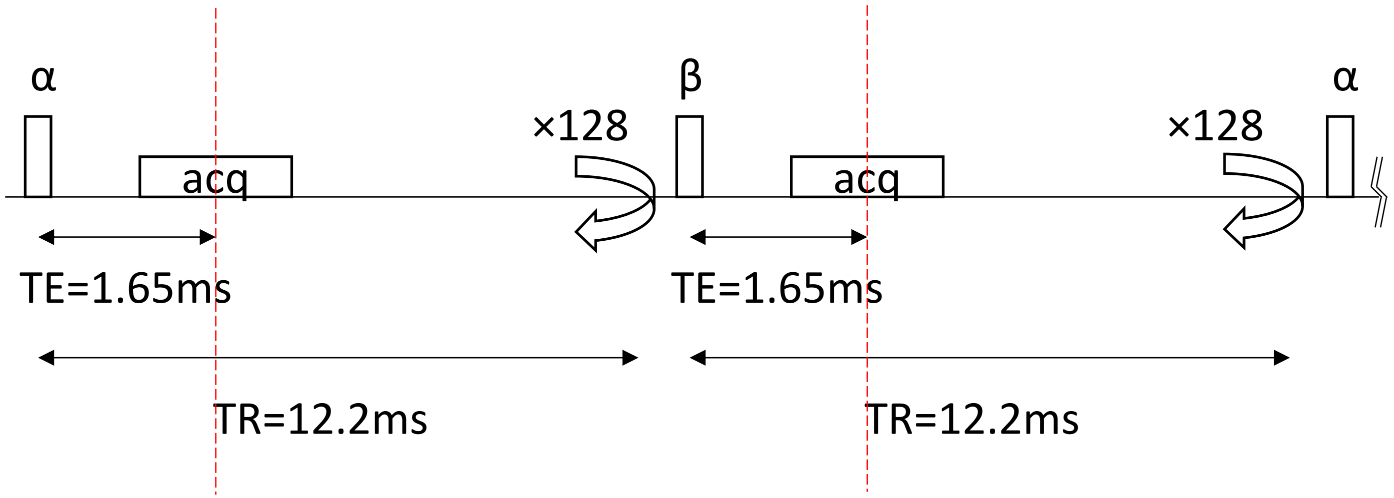

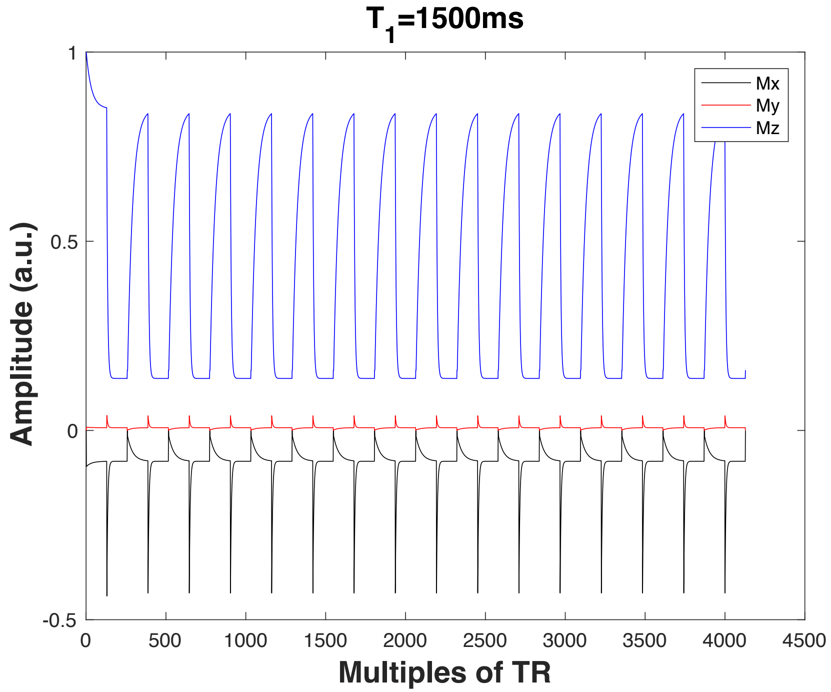

- Spoiled GRE Acquisition, TR=12.2ms, TE=1.65ms, T_2=100ms
- For spins with short T_1 (i.e. fat), SS is established much faster for both flip angles.

David Geffen School of Medicine

MR Thermometry with T_2

- Temperature dependence of T_2 has a similar origin as T_1.
- However, T_2 of water in tissue can be easily masked by other factors
- An "apparent" T_2 can be used instead to measure temperature change

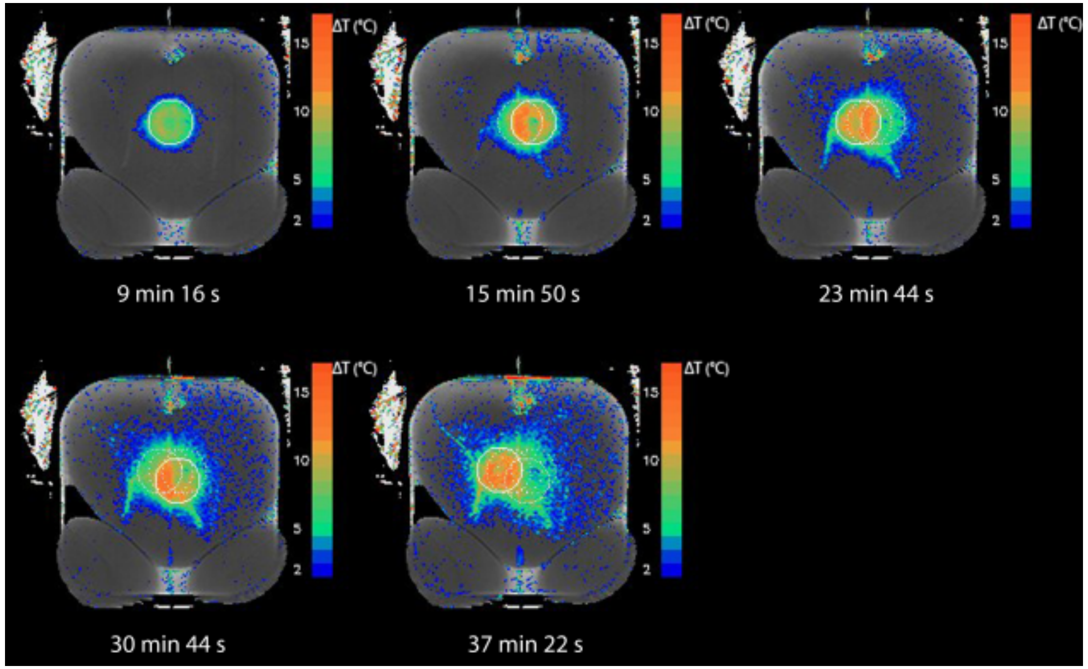

Baron P, *Magn Reson Med*. 2014

MR Thermometry with Diffusion

- Using the same approach, assuming the activation energy of free diffusion is $E_a(D)$

$$T = T_0 + \frac{kT_0^2}{E_a(D)} \frac{D - D_0}{D_0}$$

- The temperature sensitivity of ADC is high at 2%, but the acquisition time can be long, and image quality is extremely sensitive to motion
- Full diffusion tensor imaging can be necessary due to diffusion anisotropy

David Geffen School of Medicine

Rieke V, Pauly KB. J Magn Reson Imaging 2008; 27: 376-390

MR Thermometry with PRF

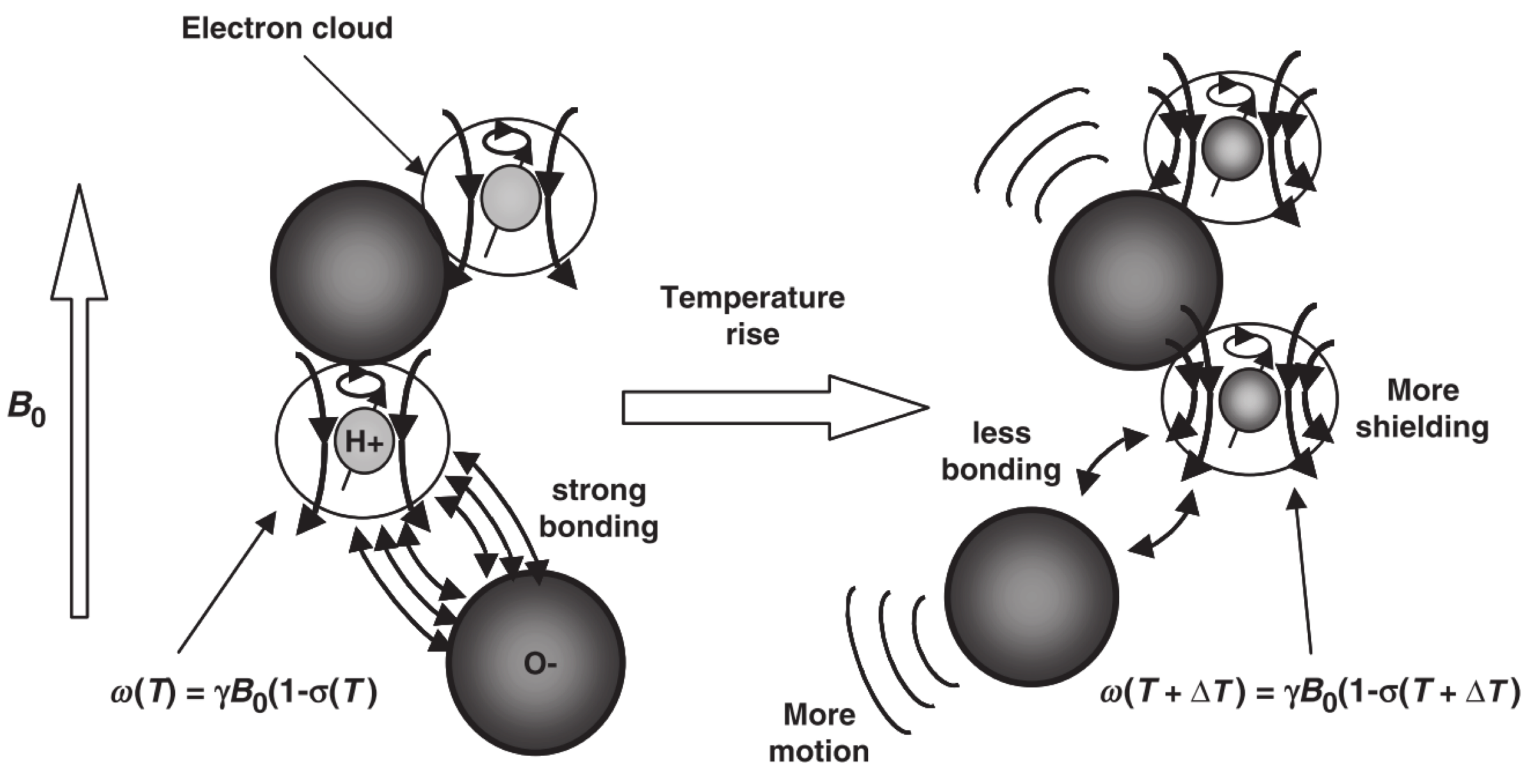

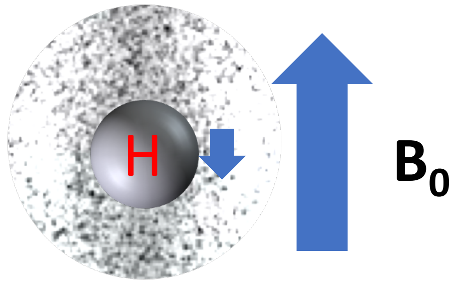

$$\omega = \gamma B_0(1 - s)$$

s is called the shielding constant, and it increases linearly with temperature between -15 and 100°C at a rate of 0.01×10^{-6}/°C as hydrogen bonds bend, twist, or break.

David Geffen School of Medicine

Kuroda K. *Int J Hyperthermia*, 2005

MR Thermometry with PRF

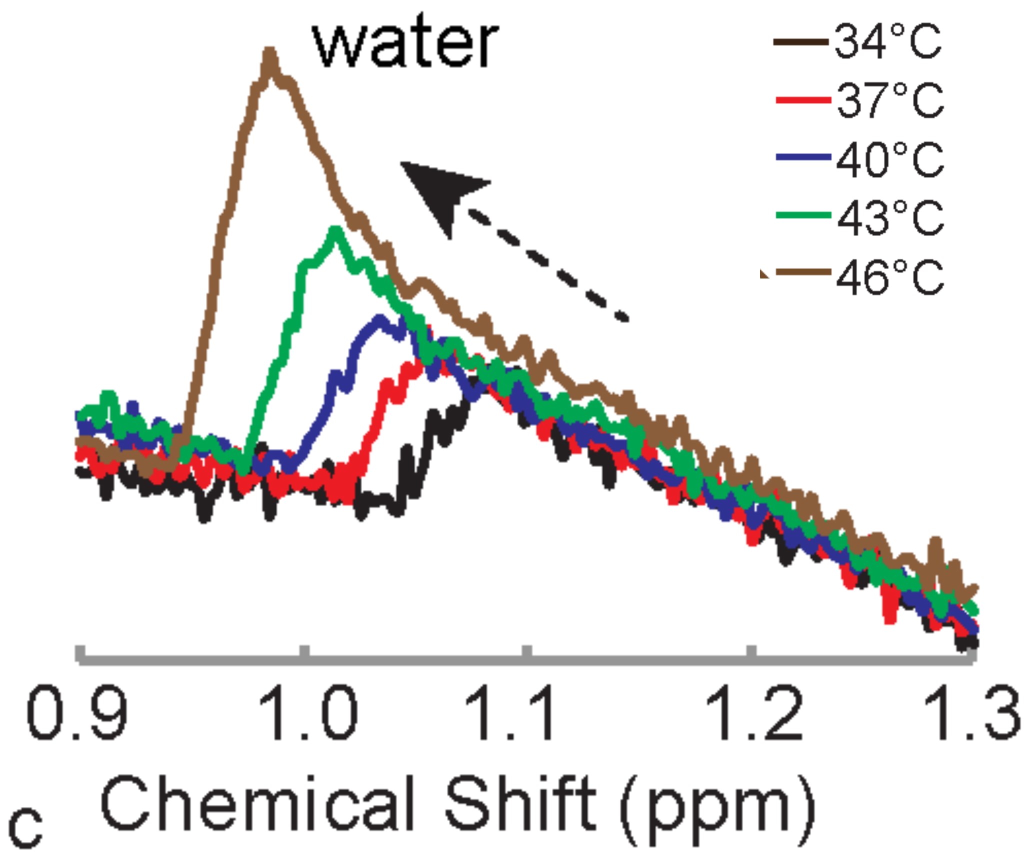

$$\Delta\phi = TE \cdot \Delta f$$

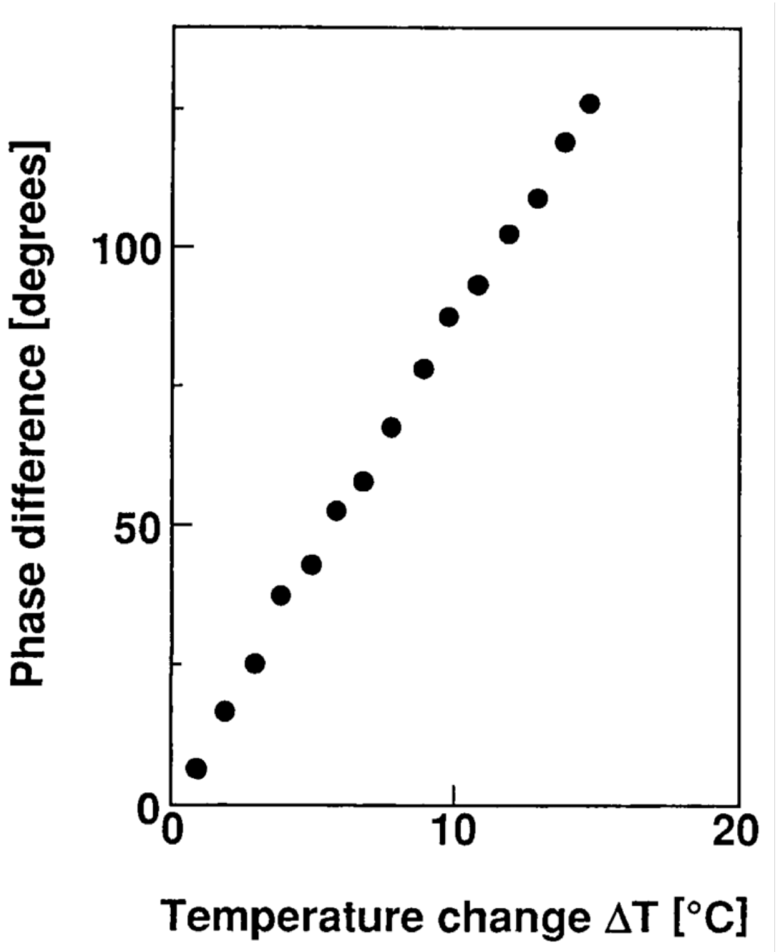

PRF Thermometry: Pitfalls

Parameter		Value	
Static magnetic field	dB0/dt	**Field drift**	0.02 ppm/h
Chemical shift	dδ/dT	**Pure water**	−0.01 ppm/°C
		Tissue (except fat)	−(0.009–0.01) ppm/°C
		Fat	−0.00018 ppm/°C
Permittivity	dε/dT	**Water**	−0.5%/°C
Electrical conductivity	$d\sigma_{el}/dT$	**Dog muscle**	1.7%/°C
Permeability	dμ/dT	**Water**	3.10−7%/°C
Magnetic susceptibility	dχ/dT	**Pure water**	0.0026 ppm/°C (30–45 °C)
		Muscle	0.0016 ppm/°C (30–45 °C)
		Breast fat	0.0039–0.0076 ppm/°C
		Air	−0.002 ppm/°C

David Geffen School of Medicine

Winter L. *Int J Hyperthermia*, 2016

MR Thermometry with PRF: Spectroscopic Approach

- A temperature independent peak is commonly used as a reference to correct for the effect of motion, field drift and/or field inhomogeneities on PRF
- This peak can be the fat (methylene) proton peak in the body, or the NAA proton peak in the brain
- Chemical shift image (CSI), echo planar spectroscopic imaging (EPSI), line scan echo planar spectroscopic imaging (LSEPI) or water saturation shift referencing methods can be used
- But this approach tends to be very slow, with poor resolution

Rieke V, *J Magn Reson Imaging*, 2008

Spectroscopic MR Thermometry with PRF

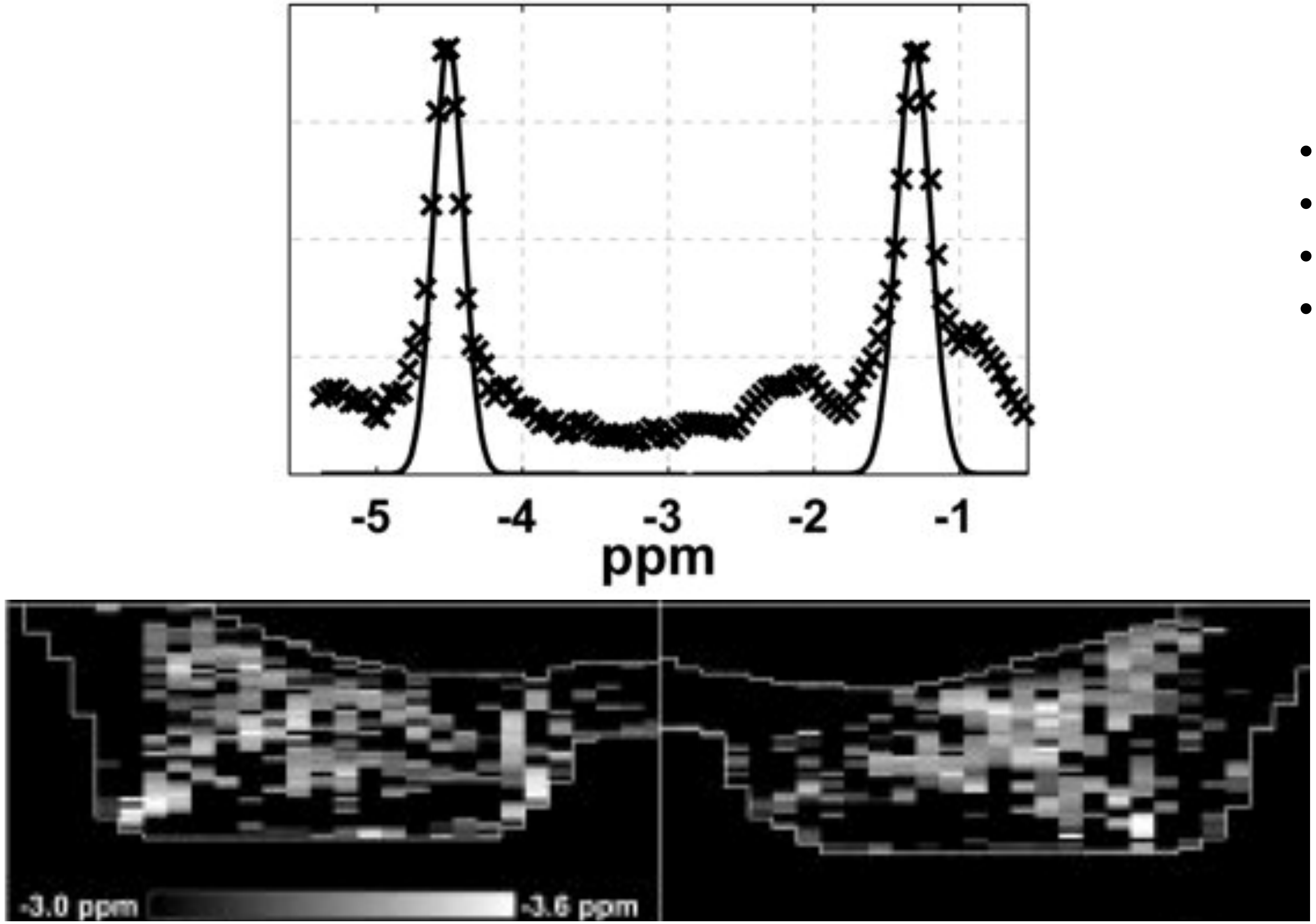

- LSEPSI method
- Human subject imaging
- 2.5*mm* in-plane resolution
- 6.5*s* scanning time per slice

David Geffen School of Medicine

MacDonnald N,. *Magn Reson Med* 2007

Spectroscopic MR Thermometry with Other Nuclei

TmDOTP5-

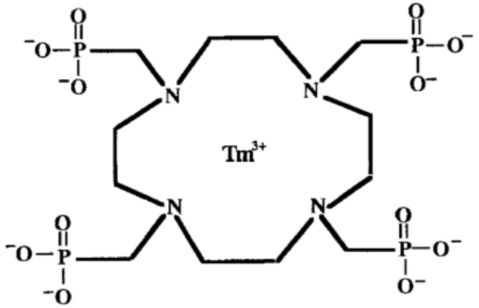

Temperature Dependence of ^{31}P Peak

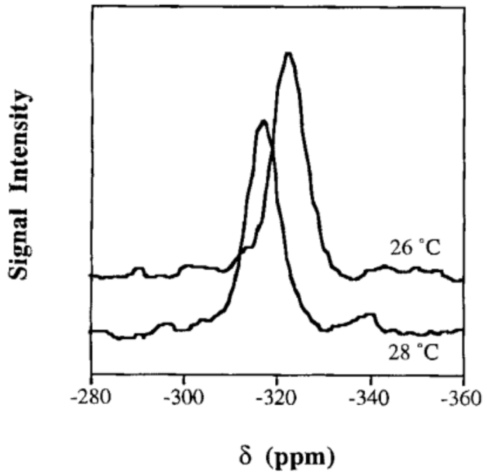

- Both ^{31}P and ^{129}Xe have higher temperature sensitivities than PRF
- Due to low natural abundance, these methods yield low SNR, long scanning time and generally are confined to spectroscopic imaging

Encapsulated ^{129}Xe

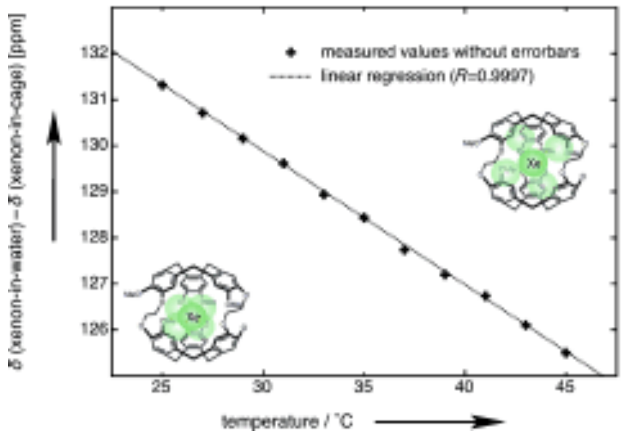

$$\delta_2[ppm] - \delta_1[ppm] = -0.29ppm/°C \times T[°C] + 138.57[ppm]$$

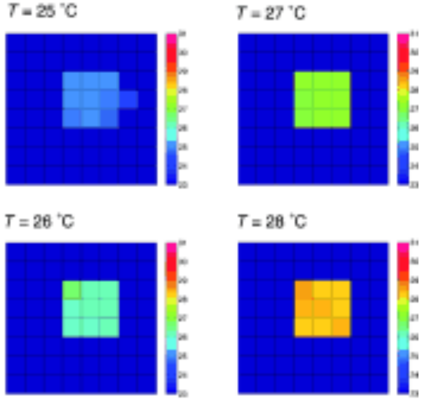

Zuo CS, *Magn Reson Med,* 1996
Schilling F, *Magn Reson Med*, 2010

Spectroscopic MR Thermometry with ^{129}Xe

- Because ^{129}Xe has a high affinity for lipid, we can potentially use fat peak as a reference

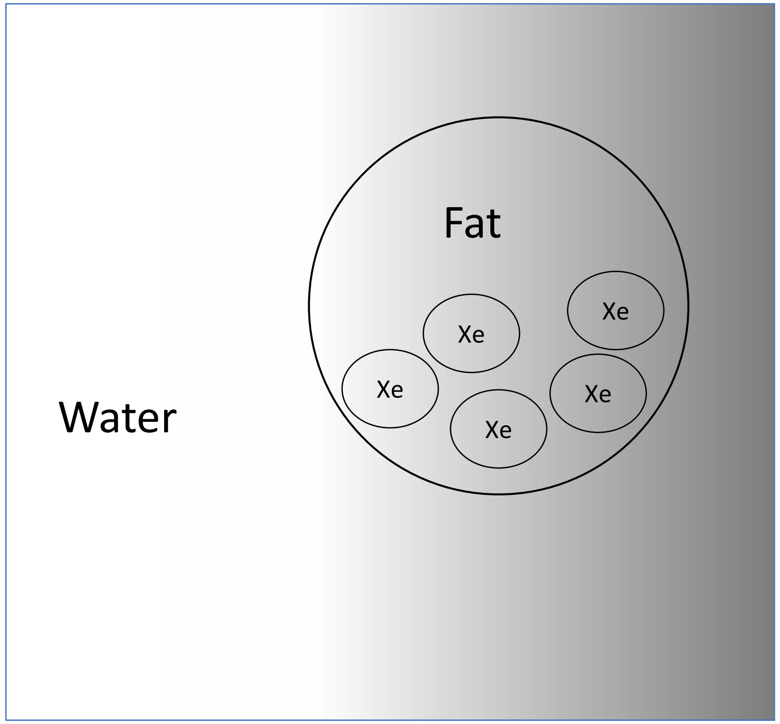

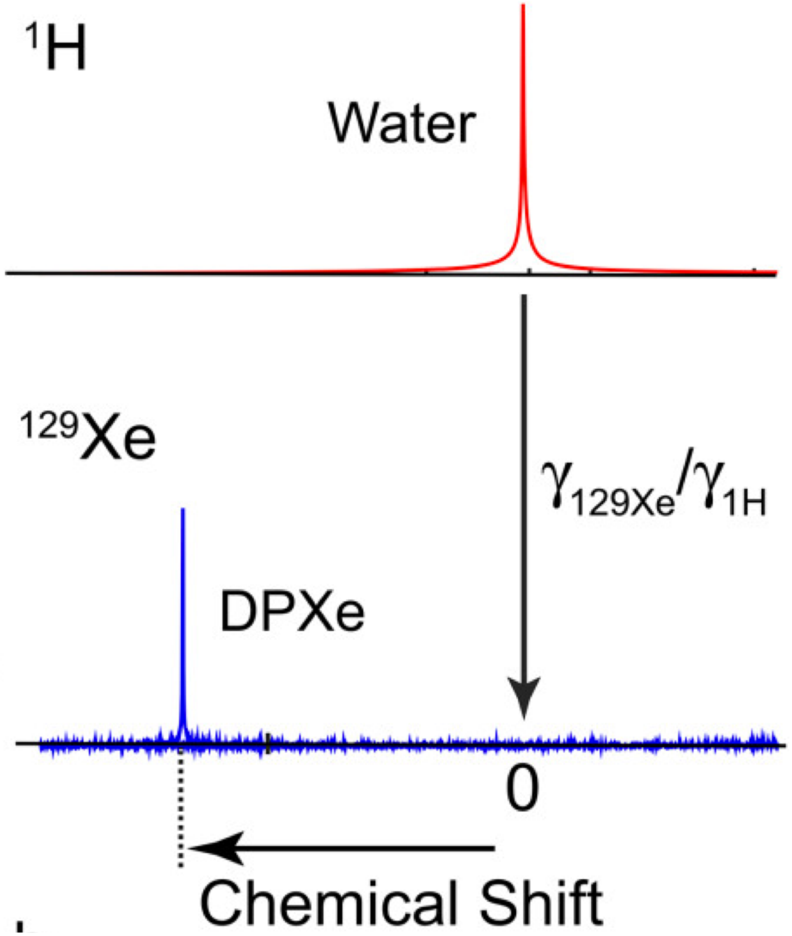

Antonacci MA, *Magn Reson Med*, 2018

Spectroscopic MR Thermometry with ^{129}Xe: Pathway Filtering

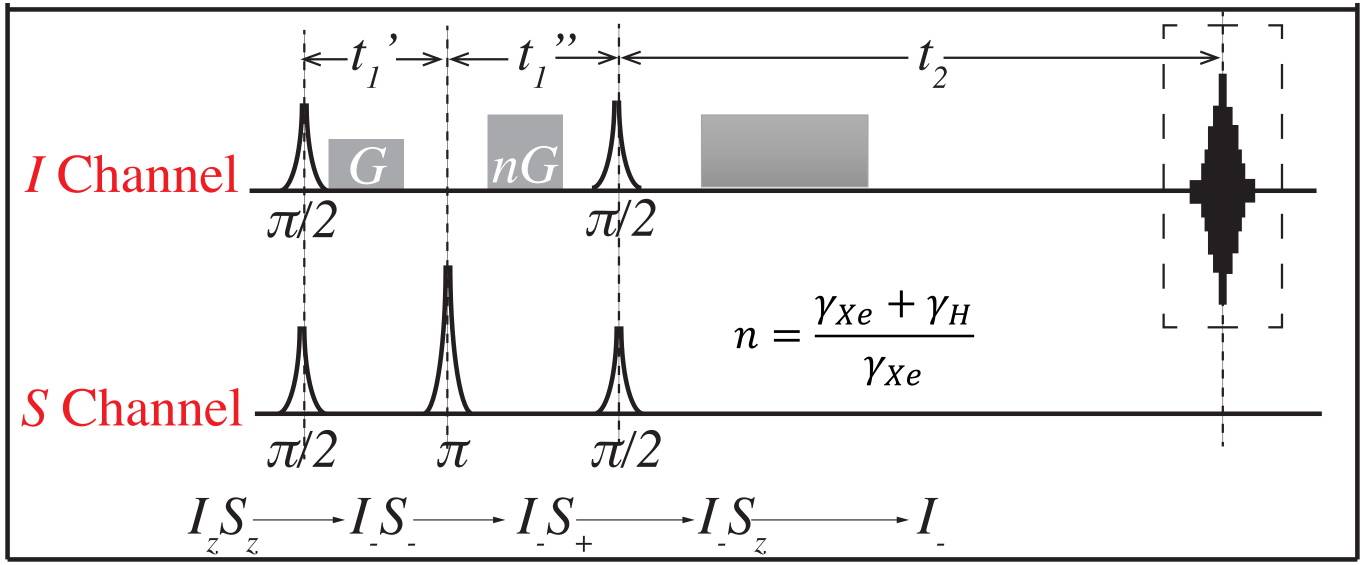

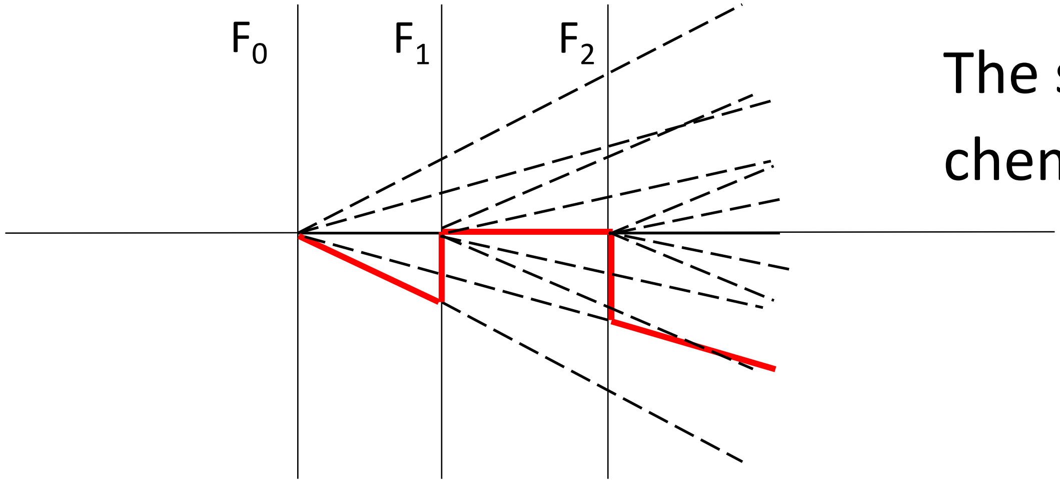

The surviving signal will have a chemical shift of $\delta_{Xe} - \frac{\gamma_{Xe}}{\gamma_H}\delta_{fat}$

David Geffen School of Medicine

Zhang L, *Magn Reson Med*, 2018

Spectroscopic MR Thermometry with ^{129}Xe: Pathway Filtering

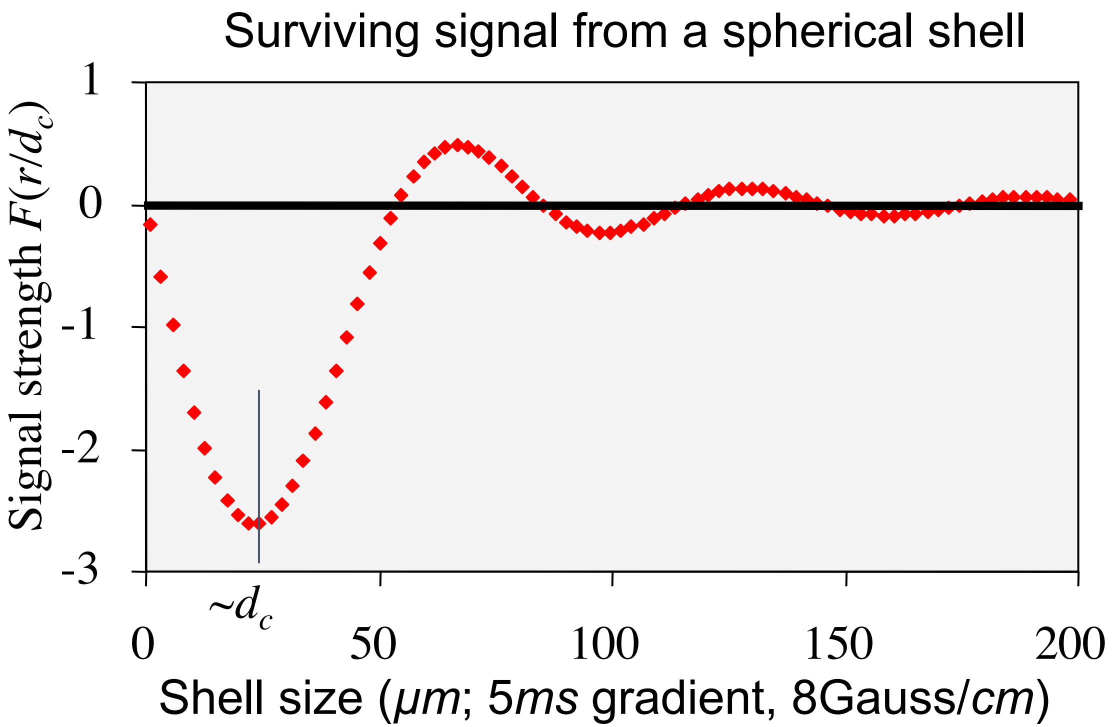

- The dipolar field makes only some of them observable

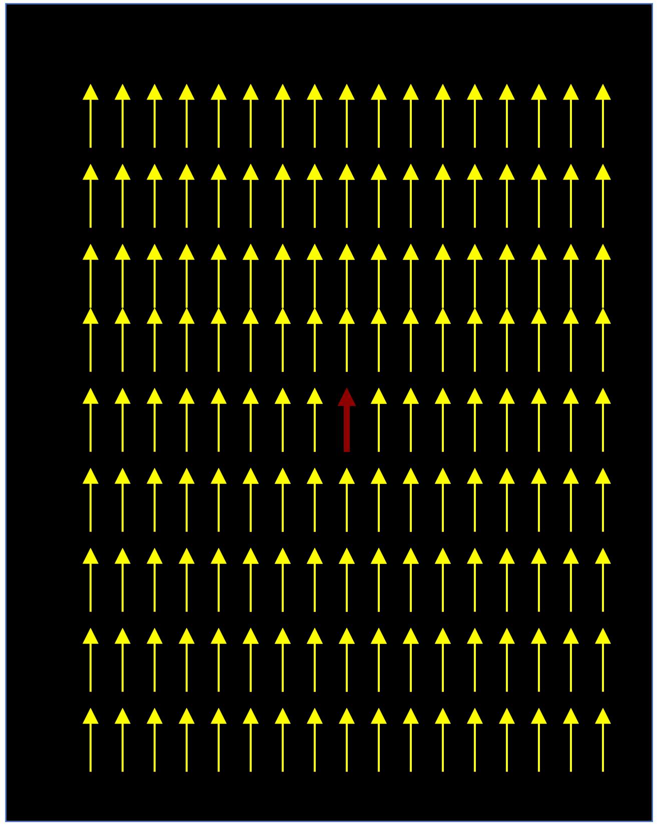

Approximate MRI Distance Scales
Direct spatial resolution (>1mm)
Surviving signal (.01-1mm)

David Geffen
School of Medicine

MR Thermometry with PRF: Phase Mapping Approach

Wrapped Phase Map

Unwrapped Phase Map

Pre-treatment temperature (or reference temperature T_0)

Unknown, elevated temperature (T)

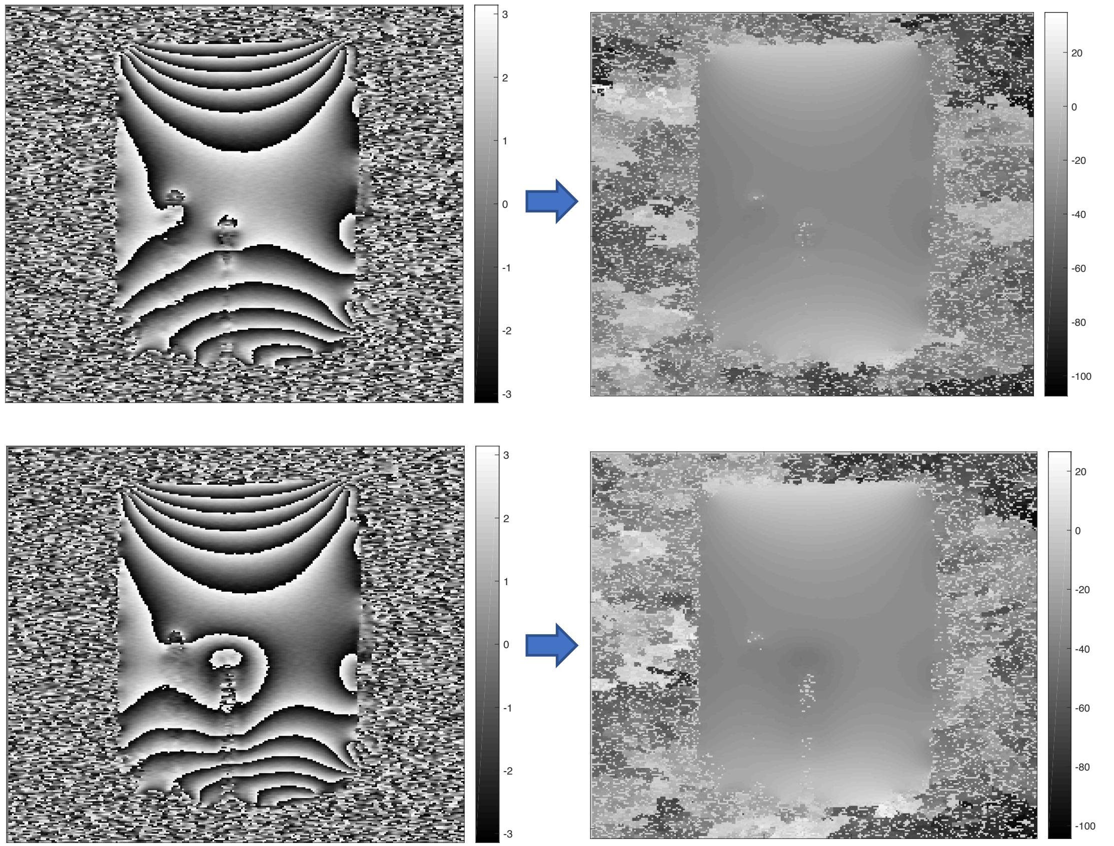

Phase Difference Map

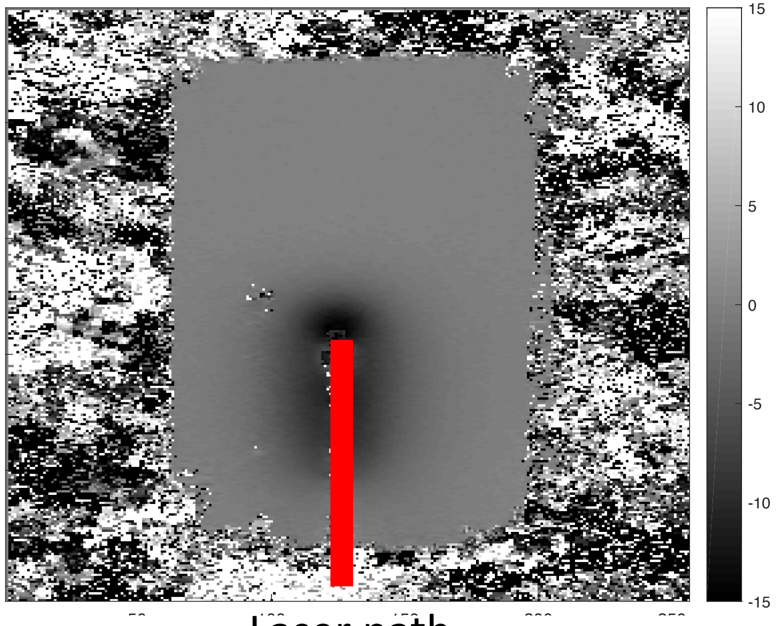

Laser path

David Geffen
School of Medicine

MR Thermometry with PRF: Phase Mapping Approach

- The estimate of T can thus be calculated as, with α=-0.01ppm/°C

Phase Difference Map

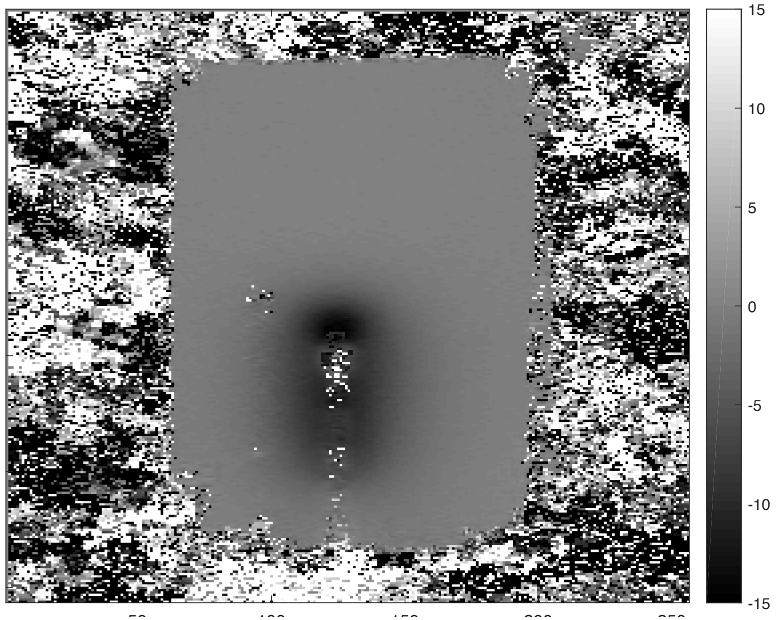

$$\Delta T = \frac{\phi(T) - \phi(T_0)}{\gamma \alpha B_0 TE}$$

Relative Temperature Change Map

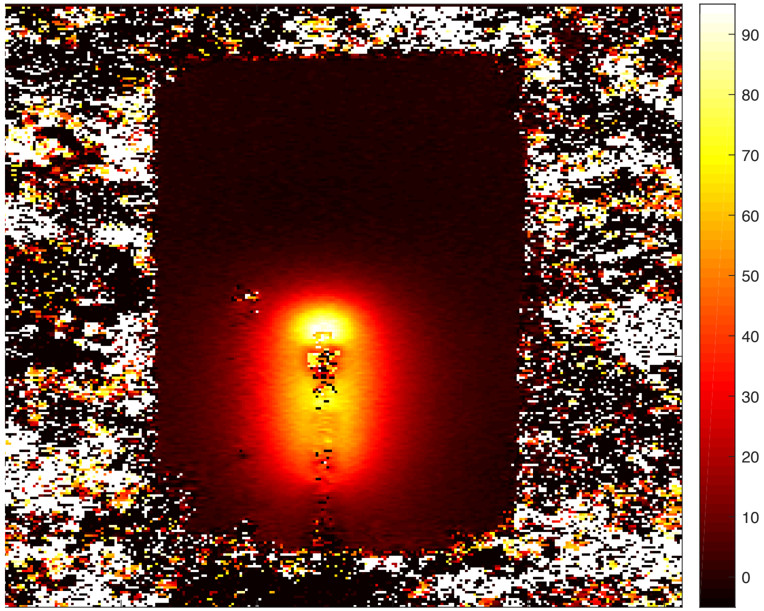

David Geffen School of Medicine

Ishihara Y, Calderon A, Watanabe H, et al. Magn Reson Med 1995; 34: 814-823

MR Thermometry with PRF: Choice of TE

Echo Time

Less relaxation; higher SNR
Lower TR; faster acquisition

More "fanning out" of the spin;
better temperature accuracy

- In a gradient echo sequence, the SNR of the phase difference between two images acquired at different temperature $\Delta\phi(\Delta T)$ is directly proportional to the signal intensity A: $SNR_{\Delta\phi} = |\Delta\phi(\Delta T)| \cdot A$
- Which is in turn: $SNR_{\Delta\phi} \propto TE \cdot e^{-TE/T_2^*}$
- Differentiating the above expression gives the optimal TE as $TE = T_2^*$

PRF Thermometry Pitfalls: Motion & Multibaseline Correction

Temperature Error due to Motion

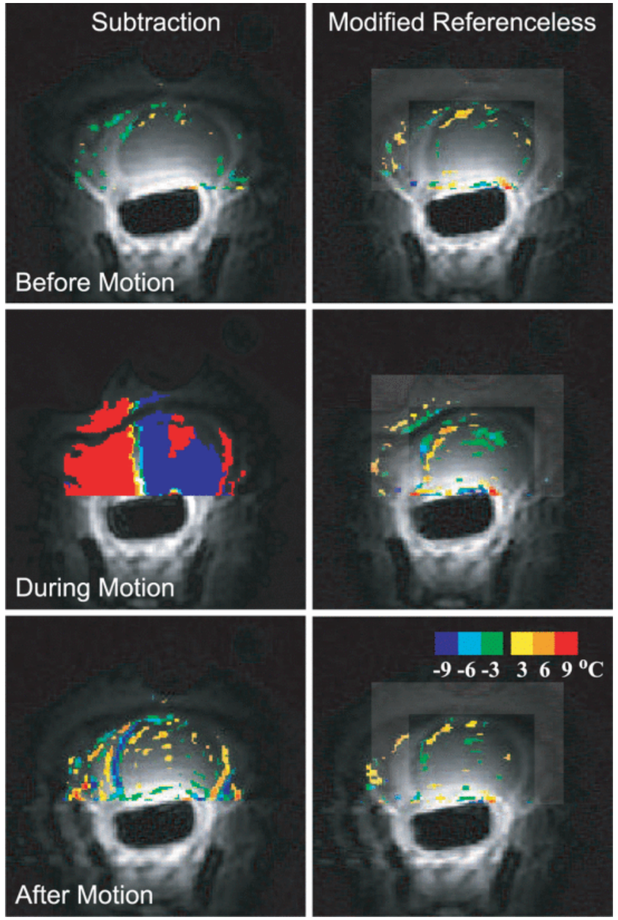

Multiple baseline images are acquired during one motion cycle

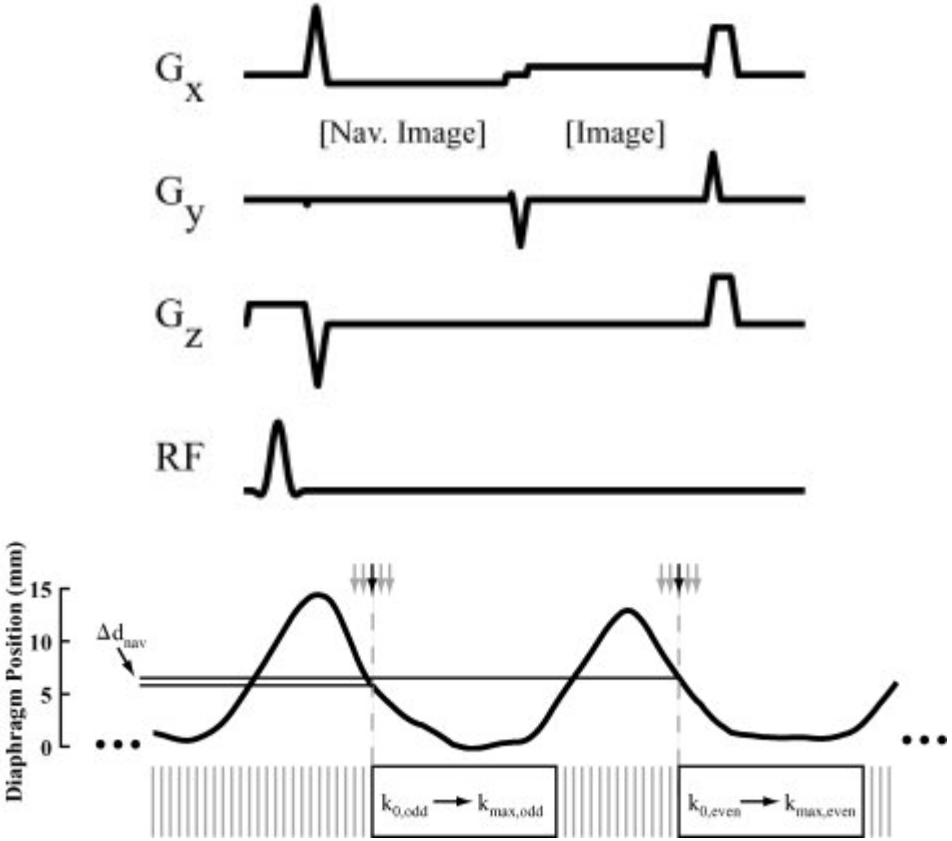

Each line in *k*-space is matched with a baseline from the library

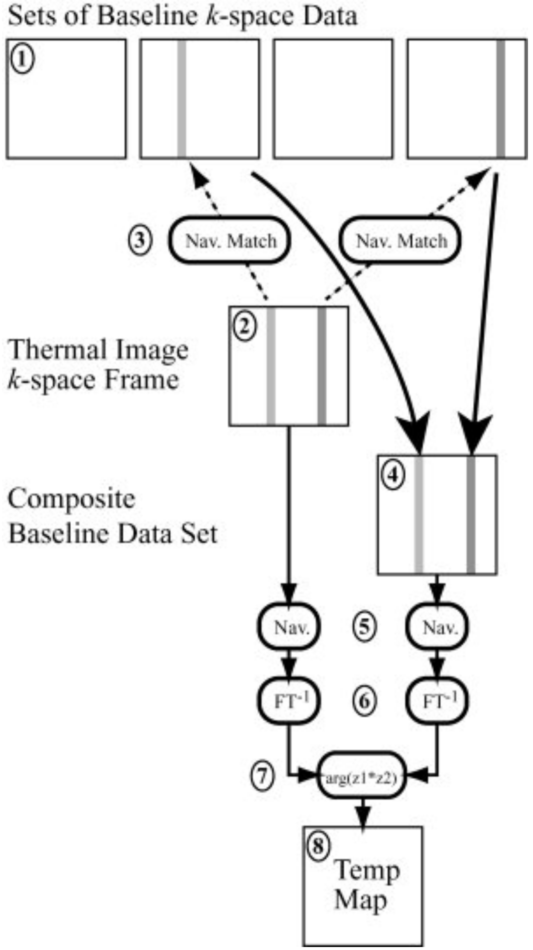

David Geffen
School of Medicine

Rieke V, *IEEE Trans Med Imaging*, 2007
Vigen KK, *Magn Reson Med*, 2003

PRF Thermometry Pitfalls: Phase of Fat

- The temperature independence of fat peak complicates phase mapping

Fat-free pixel

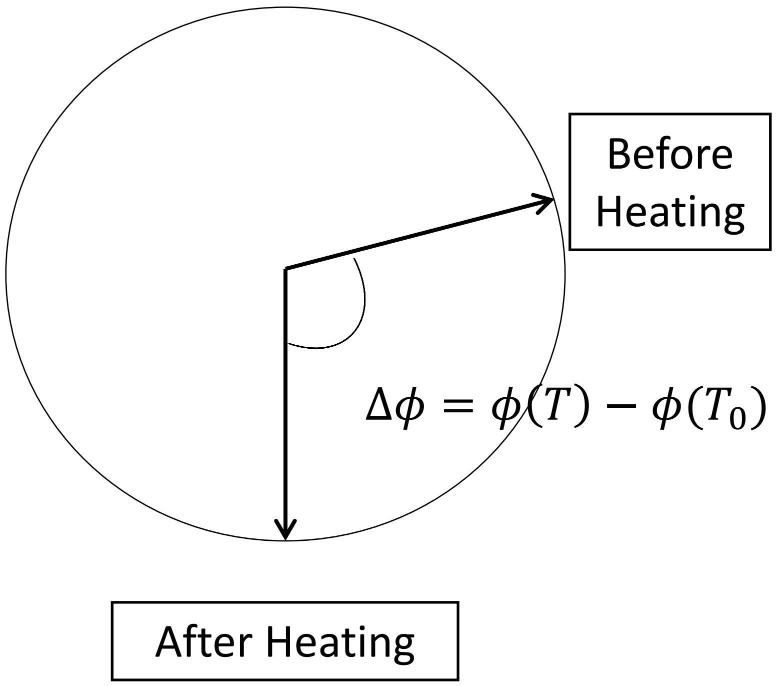

Fat-containing pixel

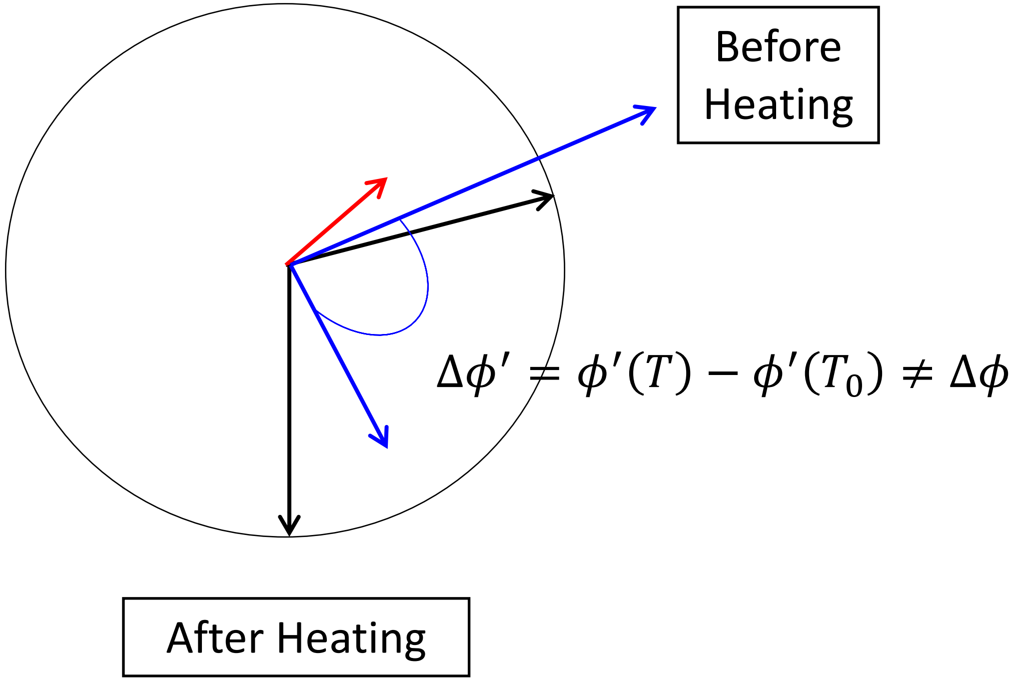

PRF Thermometry Pitfalls: Magnetic Susceptibility

- The localized magnetic field a nucleus feels deviates from the macroscopic B_0 field depending on its magnetic susceptibility

$$B_{nuc} \cong \mathrm{B}_{mac} - \left(\frac{2}{3}\chi + \sigma\right) B_0$$

- The error in temperature measurement can be

$$\epsilon_T = -\frac{1}{\alpha}\left(\frac{\Delta B_{mac}}{B_0 \Delta T} - \frac{2}{3}\frac{\Delta\chi}{\Delta T}\right)$$

- Susceptibility of fat also changes with temperature with a rate similar to PRF, further compounding the problem

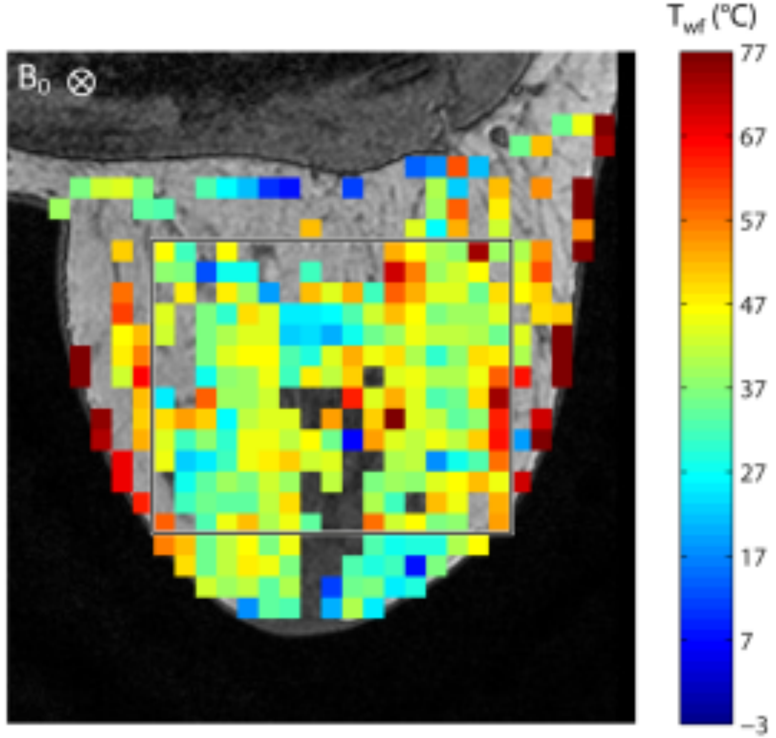

David Geffen School of Medicine

Sprinkhuizen SM, *Magn Reson Med*, 2010
Baron P, *Magn Reson Med*, 2016

PRF Thermometry with Fat: Dixon Method

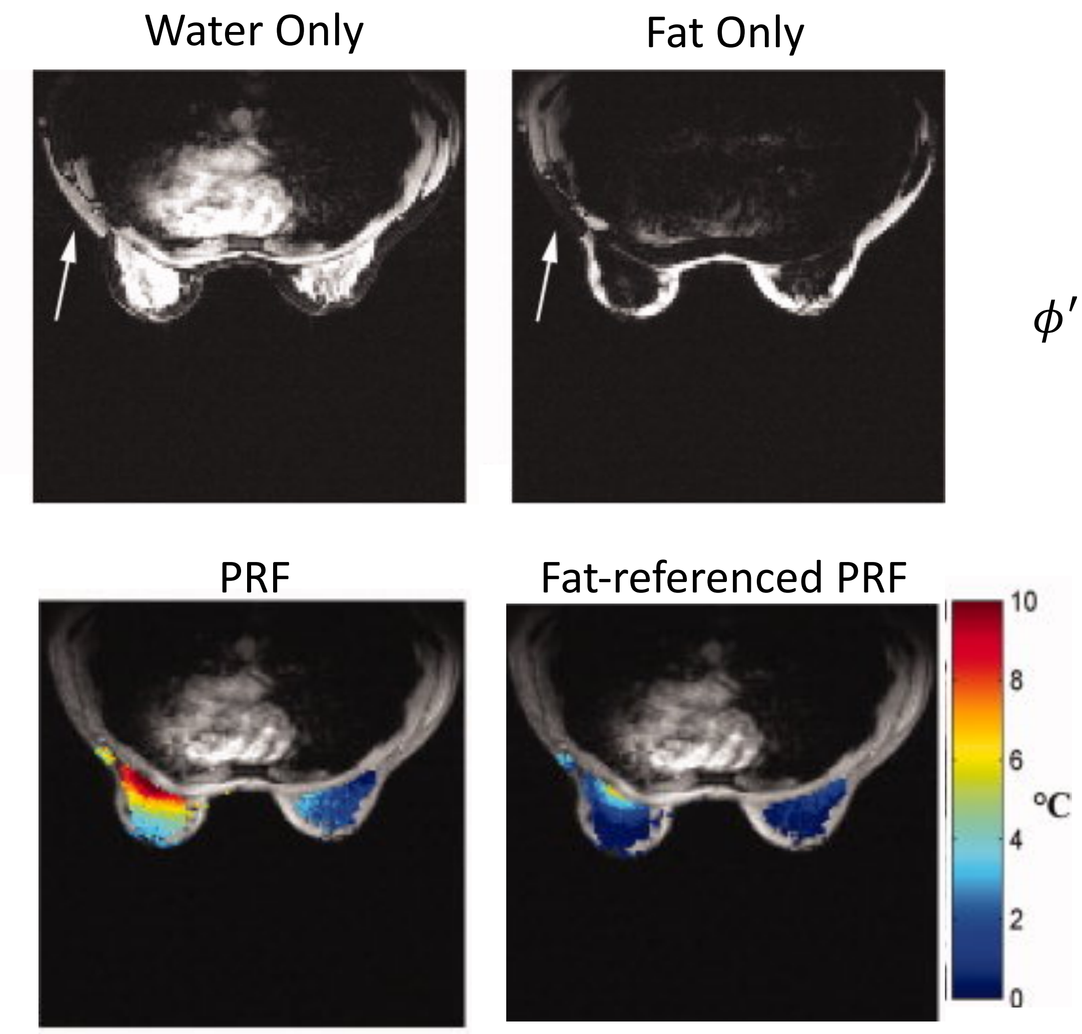

- The "fat" phase in a fat-free pixel at position (x,y) is interpolated from the phases in neighboring fat-containing pixels using a polynomial

$$\phi'(x,y) = a_0 + a_1 x + a_2 y + a_3 x^2 + a_4 y^2 + a_5 xy + \cdots$$

and this phantom reference is used to correct for the PRF phase change in that pixel

- In fat-containing pixels, the phase at a known temperature is subtracted from the phase at the elevated temperature. The net phase change is assumed to be purely caused by PRF

David Geffen School of Medicine

Hofstetter LW, *J Magn Reson Imaging*, 2012

PRF Thermometry with Fat: Hybrid PRF/T_1

- Three-point Dixon images separate water and fat compartments
- GRE multiple echoes are combined to generate phase maps at each time step to produce temperature maps with PRF in water compartments
- T_1 is measured using variable flip angle (VFA) method to produce temperature maps in fatty compartments

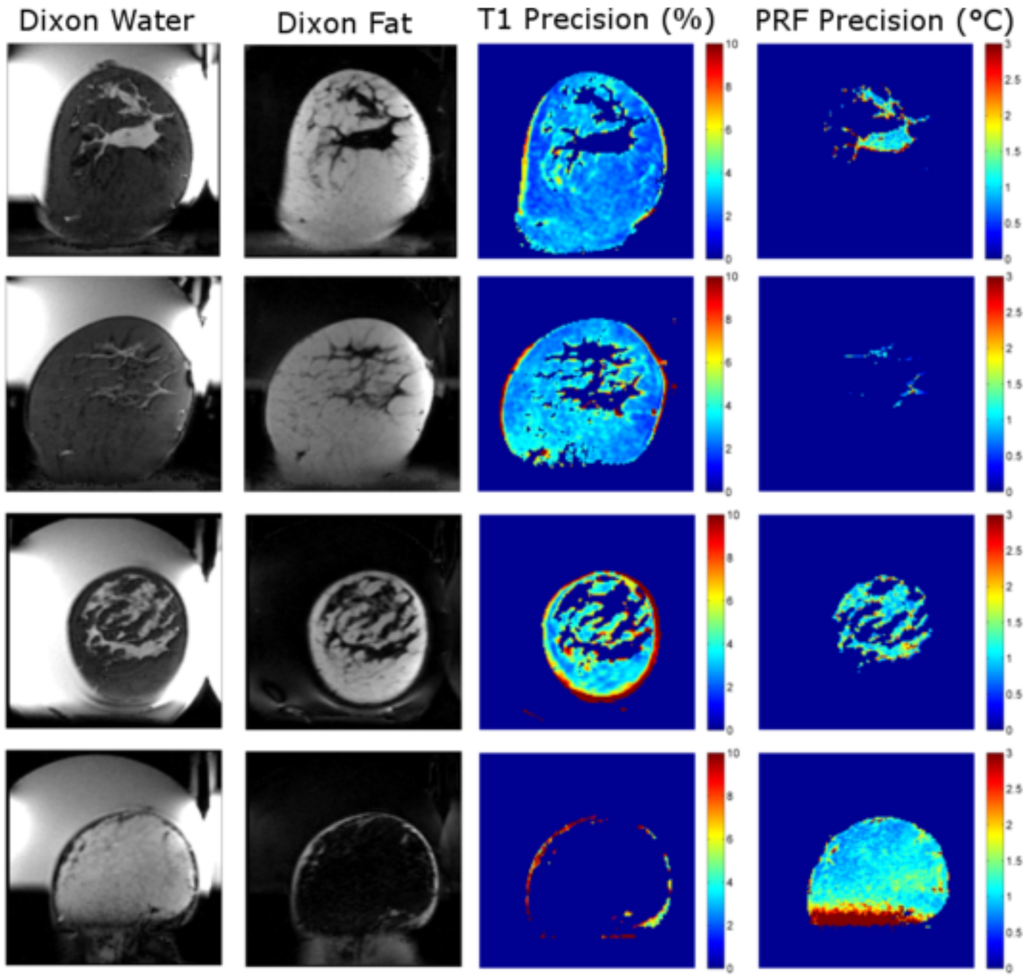

David Geffen
School of Medicine

Todd N, *Magn Reson Med*, 2014

PRF Thermometry with Fat: Referenceless

- Assuming a small heated region and a smooth-changing baseline phase map

$$\phi_b(x, y) = \Sigma_{n=0}^{N}\Sigma_{m=0}^{n-1} a(m, n) f_{m-n}(x) f_n(y)$$

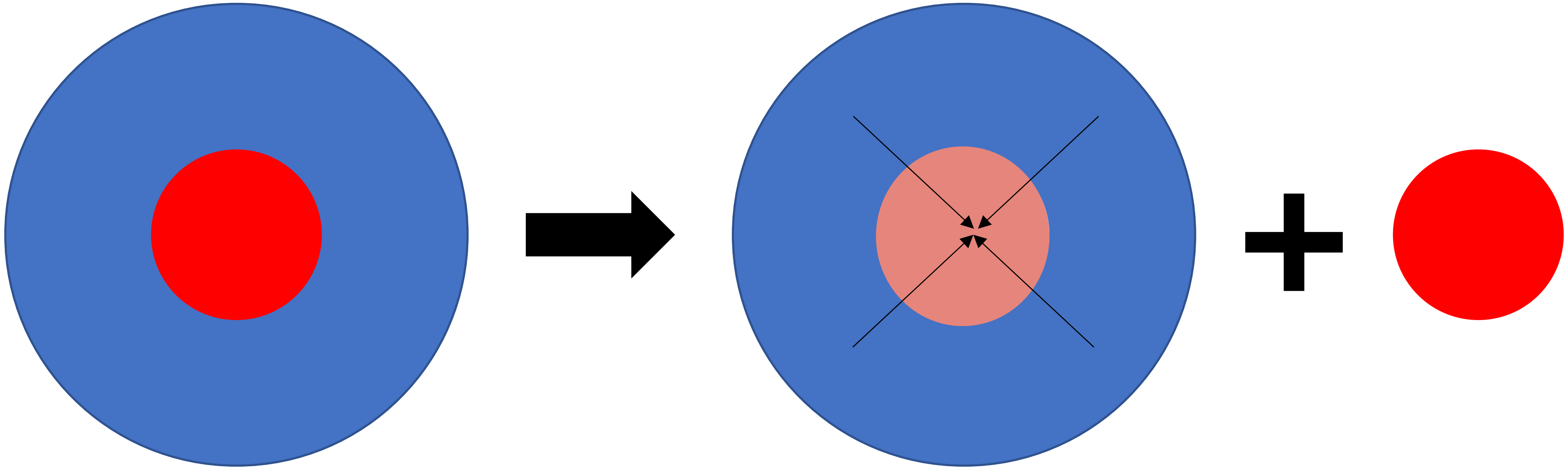

Rieke V, *Magn Reson Med*, 2004

Referenceless PRF Thermometry: Phase Gradient without Phase Unwrapping

- The gradient of the phase map along both *x* and *y* directions is expanded into a polynomial

$$\nabla_x \phi_e(x,y) = \Sigma_{n=0}^{N} \Sigma_{m=0}^{n-1} a_x(m,n) f'_{m-n}(x) f_n(y)$$

- The coefficients $a_x(m,n)$ are then solved for by minimizing the ℓ_2 norm of

$$\min_{a_x(m,n)} \Sigma_x \Sigma_y w(x,y) \left(\Delta_x \phi(x,y) - \Delta_x \phi_e(x,y) \right)^2$$

- The baseline phase map is then obtained by integrating the coefficients

David Geffen School of Medicine

Langley J, *Phys Med Biol*, 2011

Referenceless PRF Thermometry: Reweighted ℓ_1 without ROI

- ℓ_1 regression is used to minimize the influence of outliers (much smaller hot spot): $\hat{\boldsymbol{a}} = \underset{\boldsymbol{a}}{\operatorname{argmin}} \Sigma_{n=1}^{N_s} ||I(x_n, y_n)|(\theta_n - \{\boldsymbol{Xa}\}_n)|$
- After each step the image is reweighted to minimize the impact of the hot spot on the overall fit

$$l = 0, \boldsymbol{W}^0 = \operatorname{diag}(|I(x_n, y_n)|)$$

$$\hat{\boldsymbol{a}}^l = \underset{\boldsymbol{a}}{\operatorname{argmin}} \parallel \boldsymbol{W}^l(\boldsymbol{\theta} - \boldsymbol{Xa}) \parallel_1$$

until l=l_{max}

$$\boldsymbol{r} = \boldsymbol{\theta} - \boldsymbol{X}\hat{\boldsymbol{a}}^l$$

$$\boldsymbol{W}^{l+1} = \operatorname{diag}\left(\frac{|I(x_n, y_n|}{|r_n| + 0.01}\right)$$

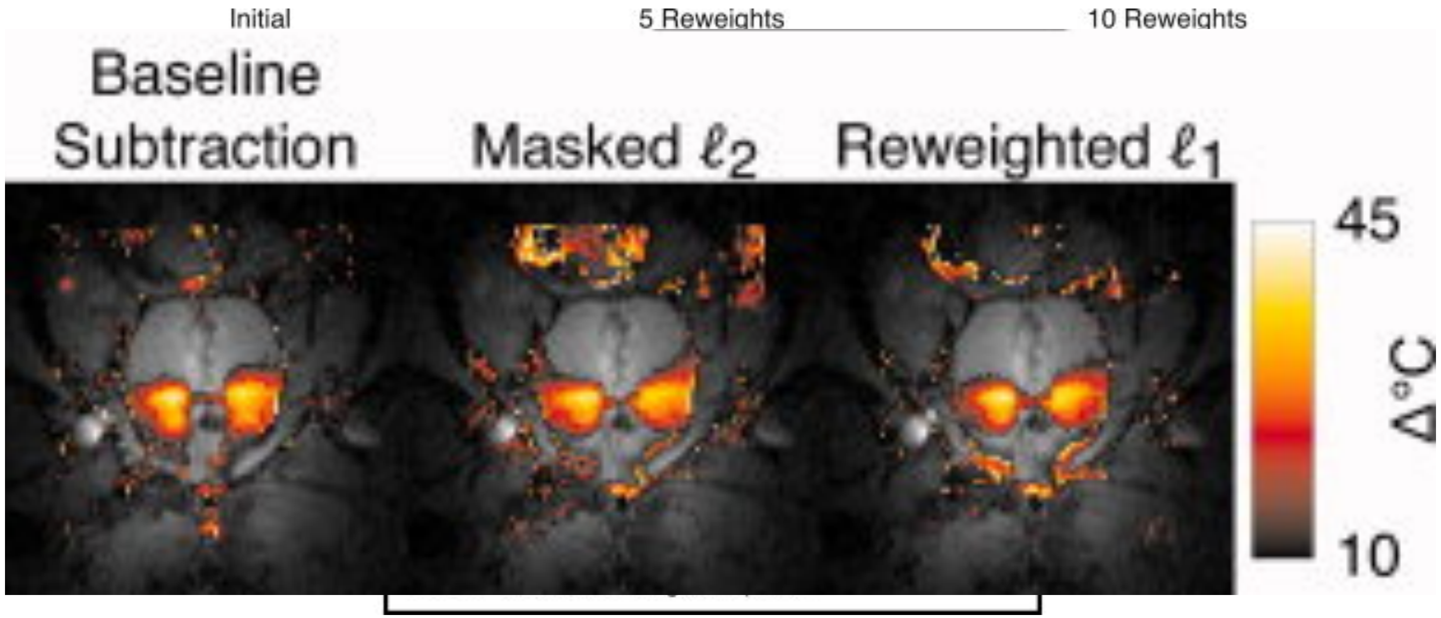

Grissom WA, *Magn Reson Med*, 2010

More Advanced MR Thermometry Methods: Hybrid Referenceless/Multibaseline Subtraction

- The model for image voxel *j* during treatment is

$$y_j = \left(\sum_{b=1}^{N_b} x_{b,j} w_b\right) e^{i(\{Ac\}_j + \theta_j)} + \epsilon_j$$

- Iterative regularized temperature estimation is conducted to find a combination of *w*, *c* and *ϑ* that minimizes a cost function

$$\Psi(w, c, \theta) = \frac{1}{2} \sum_{j=1}^{N_s} \left| y_j - \left(\sum_{b=1}^{N_b} x_{b,j} w_b\right) e^{i(\{Ac\}_j + \theta_j)} \right|^2 + \lambda \parallel \theta \parallel_0$$

Baseline library

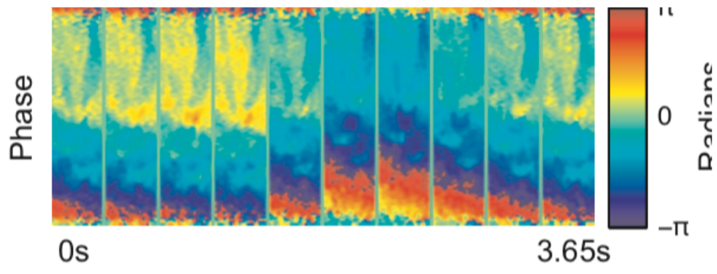

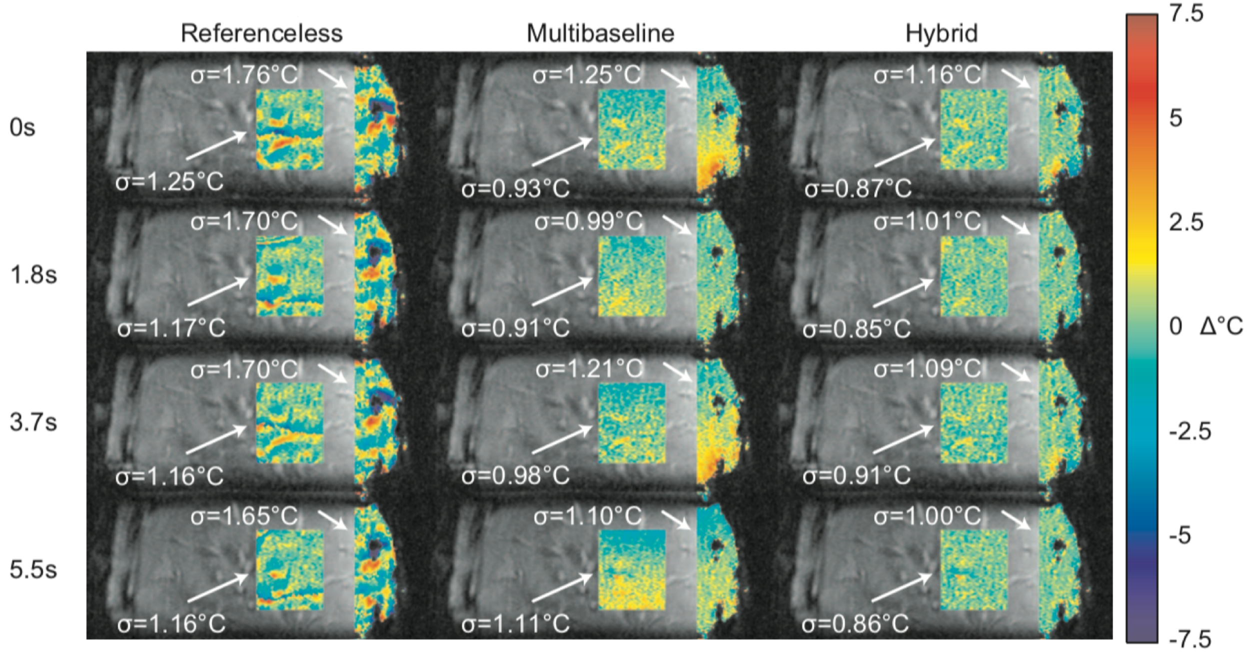

David Geffen School of Medicine

Grissom WA, *Med Phys*, 2010

More Advanced MR Thermometry Methods: Multipathway

- Dual pathway method acquires PSIF (p=-1) at earlier time point during TR and FISP (p=0) at later time point to maximize TNR
- Temperature sensitivity of pathway p is

$$\Lambda_p = (\gamma \alpha B_0) \times (pTR + TE_p)$$

- The relative temperature changes from both pathways are combined using a weighted sum method

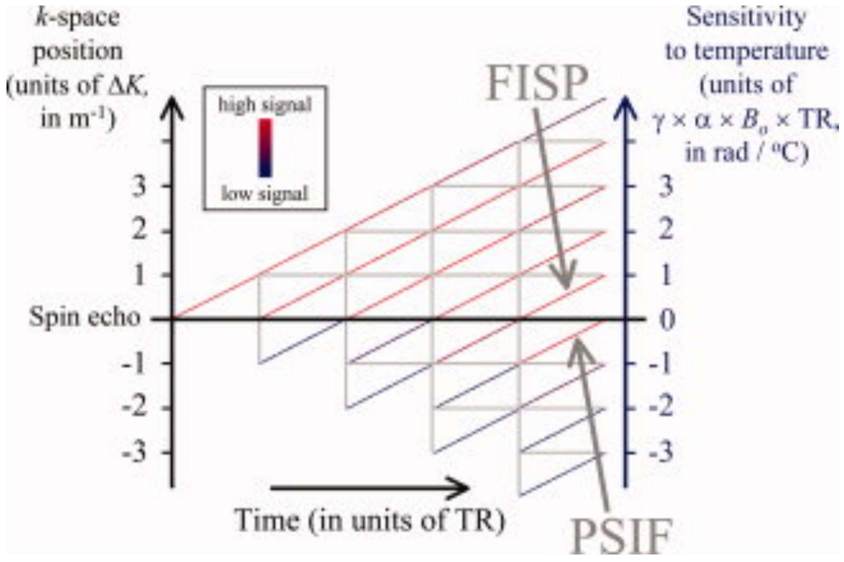

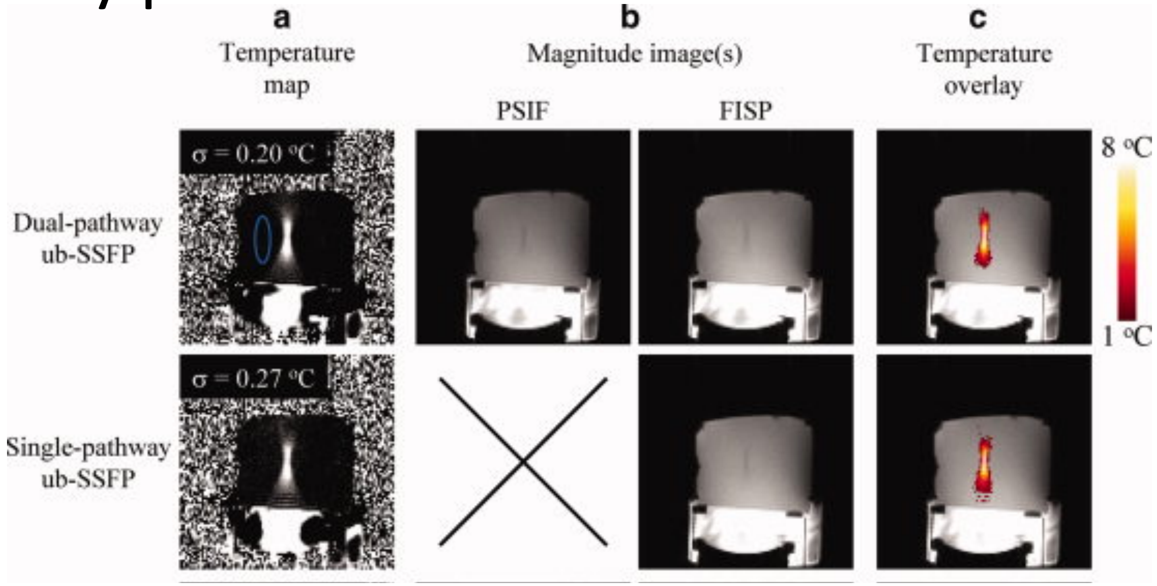

Madore B, *Magn Reson Med*, 2011

More Advanced MR Thermometry Methods: Volumetric

Excitation and acquisition of all slices in one TR

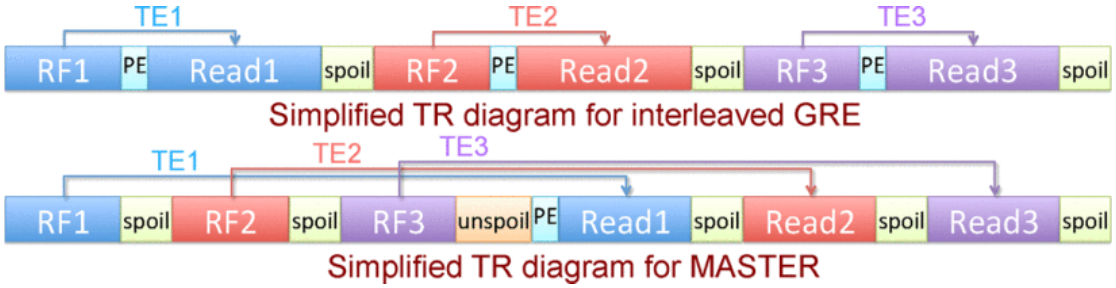

Slice Ordering

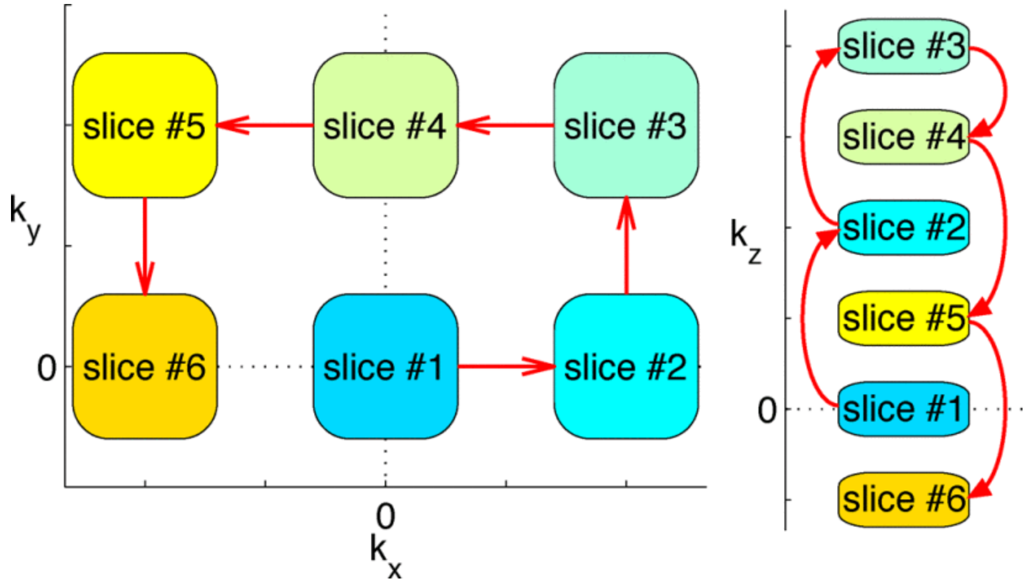

- Spoiler gradients along x and y ensure spatial separation of different slices in *k* space

Sequence performance compared with multi-slice GRE

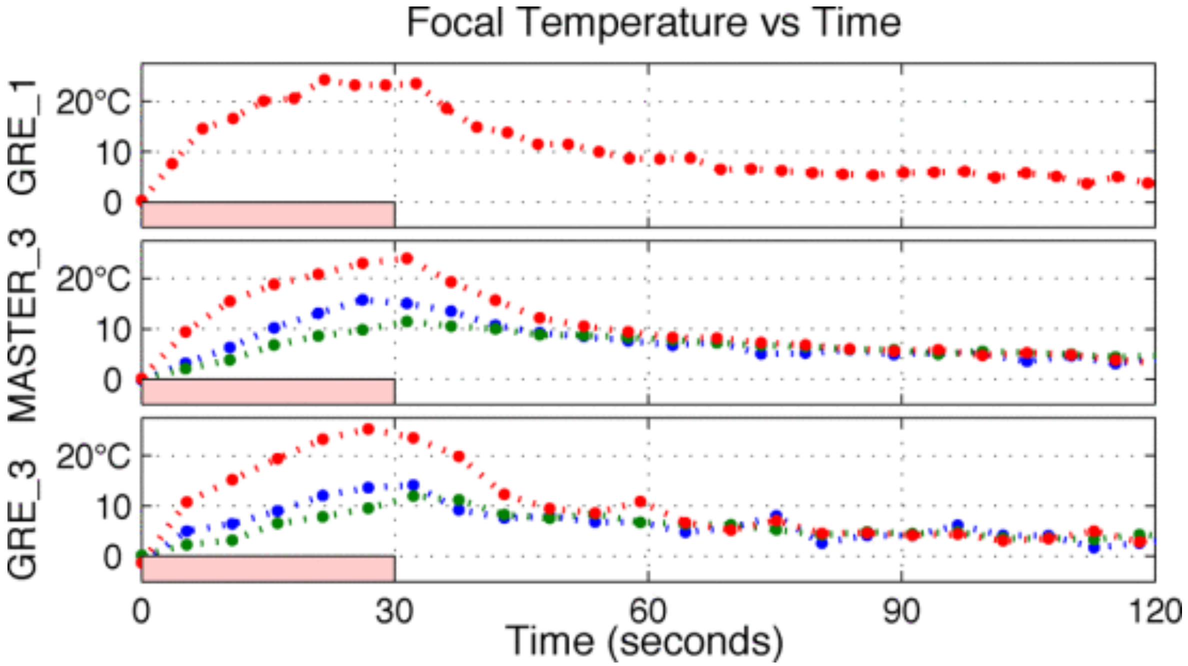

Marx M, *IEEE Trans Med Imaging*, 2015

More Advanced MR Thermometry Methods: Undersampling & TCR

Fully sampled *k*-space: *d*

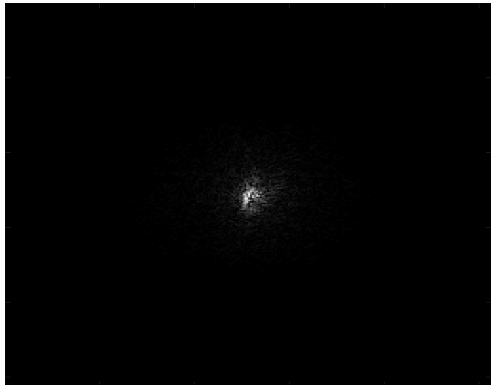

FFT

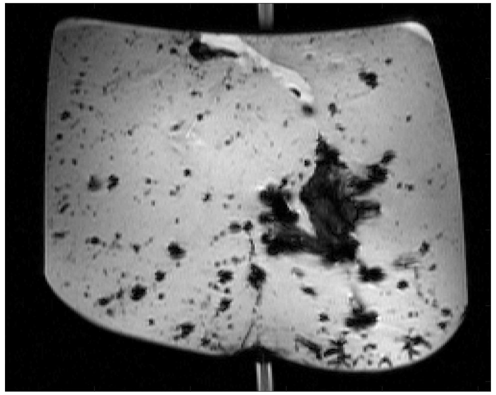

Unaliased image: *m*

Undersampled *k*-space: *d'*

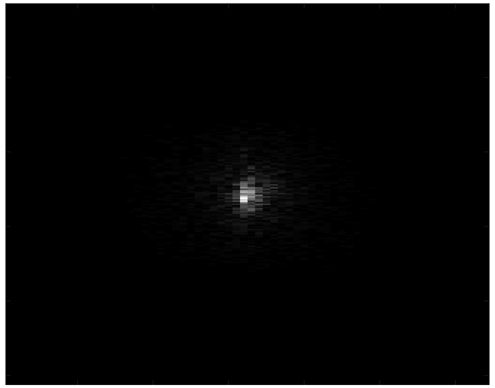

FFT

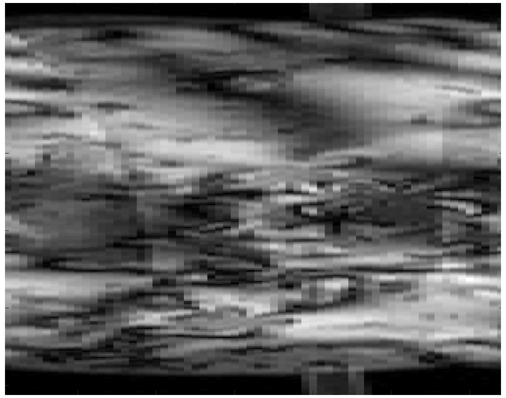

Aliased image: *m'*

- The cost function includes a fidelity term and a temporal constraint term

$$m^* = \underset{\tilde{m}}{\operatorname{argmin}}(\| WF\tilde{m} - d' \|_2^2 + \alpha\psi(\tilde{m}))$$

- For MR thermometry

$$\psi(\tilde{m}) = \sum_i^N \| \sqrt{(\nabla_t \widetilde{m_i})^2 + \beta^2} \|_1$$

Estimated image: $\tilde{m}$

Todd N, *Magn Reson Med*, 2009

David Geffen School of Medicine

More Advanced MR Thermometry Methods: Golden Angle Volumetric

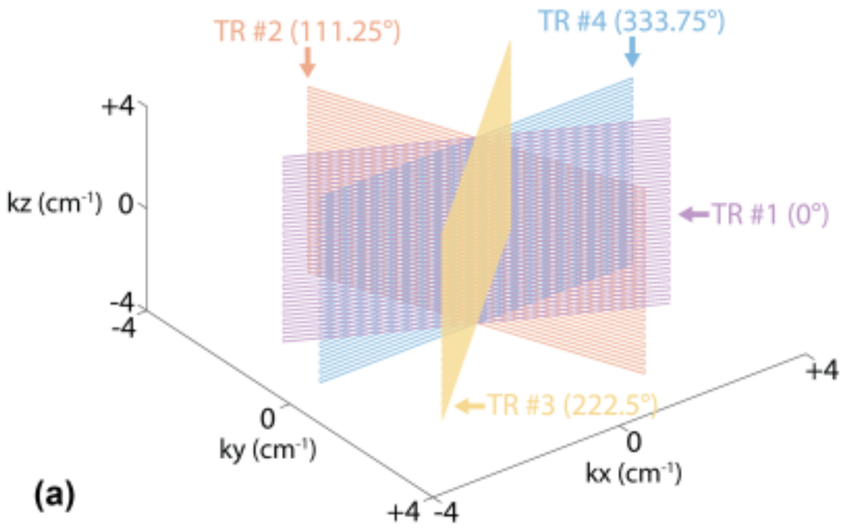

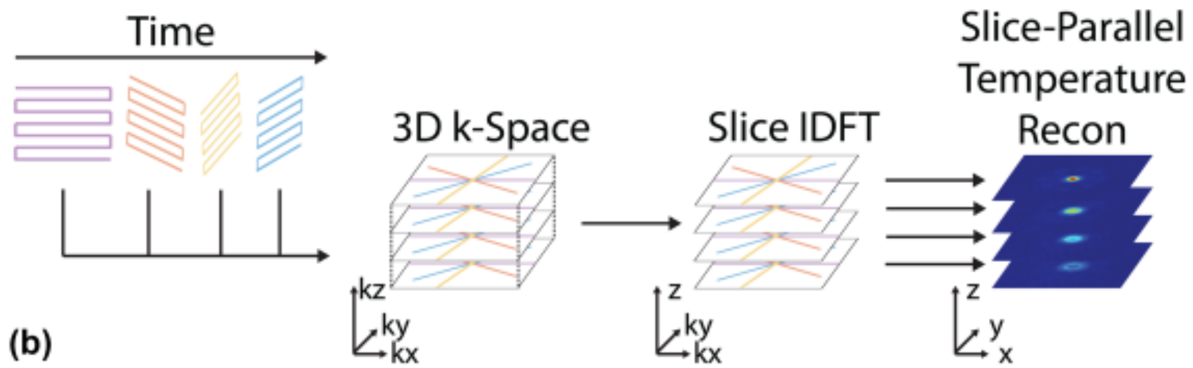

- In-plane golden angle radial encoding and through-plane Cartesian EPI encoding
- Temperature map is generated using both hybrid multibaseline/referenceless and k-space direct estimation methods

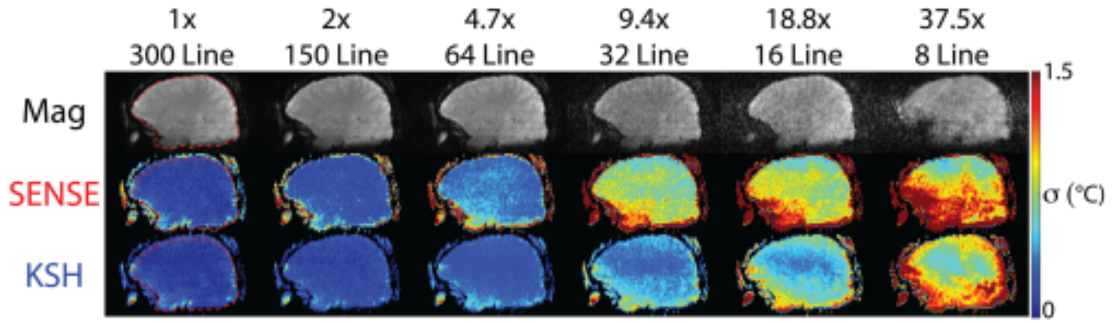

David Geffen School of Medicine

Jonathan SV, *Magn Reson Med*, 2017

More Advanced MR Thermometry Methods: Stack of Stars

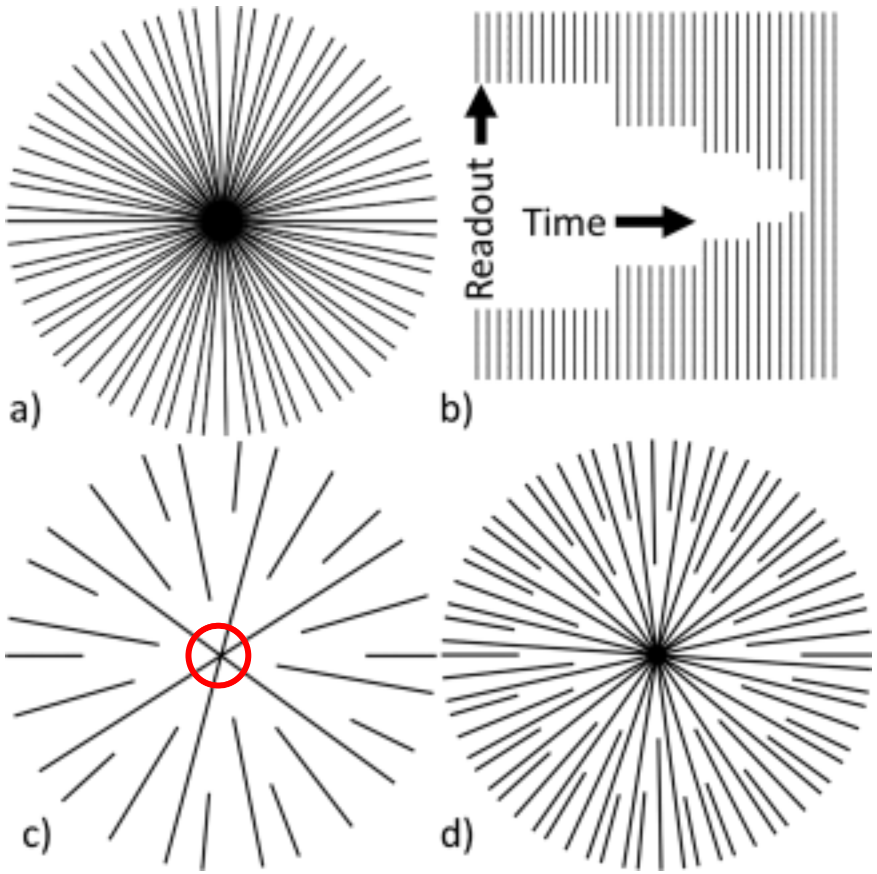

- Dipolar gradient echo acquisition scheme allows every k-space encoding step to traverse from one edge of k-space through the center to the other edge. The spoke is then rotated by the golden angle (137.56°) until sufficient coverage of k-space is met.
- Since the center of *k*-space line is acquired every TR, it has a natural robustness to motion. The k-space center can also be used as a navigator for motion correction.

Svedin BT, *Magn Reson Med*, 2017

Summary

- MR thermometry has been successfully implemented in multiple clinical studies, including breast, prostate, liver and rectal cancer.
- Various methodologies for better and faster temperature measurement using MRI are presented here. PRF still remains the most robust method, but combining PRF with T1 has also yielded promising results in mixed muscle and fatty tissues. The sensitivity of the PRF method to motion, perfusion and susceptibility changes, as well as the inability to measure temperatures in fatty tissue, are remaining challenges to improving accuracy and expanding its clinical potential.